Article:
Aad, G., Aakvaag, E., Abbott, B. et al. (2026) Measurement of the top-quark Yukawa coupling from tt production in the lepton+jets final state using pp collisions at √s = 13 TeV with the ATLAS detector. Journal of High Energy Physics, 2026. 117.

https://doi.org/10.1007/jhep01(2026)117

Published for SISSA by Springer

Received: *September 22, 2025*
Accepted: *November 8, 2025*
Published: *January 19, 2026*

Measurement of the top-quark Yukawa coupling from $t\bar{t}$ production in the lepton+jets final state using pp collisions at $\sqrt{s} = 13$ TeV with the ATLAS detector

The ATLAS collaboration

Full author list at the end of the paper

E-mail: atlas.publications@cern.ch

Abstract: The top-quark Yukawa coupling is extracted from the distribution of the top-quark pair ($t\bar{t}$) invariant mass in proton-proton collisions using 140 fb^{-1} of data at $\sqrt{s} = 13$ TeV collected in 2015–2018 by the ATLAS experiment at the Large Hadron Collider. In the region near the production threshold, the $t\bar{t}$ invariant mass spectrum is sensitive to electroweak virtual corrections, including contributions from Higgs boson exchange, thereby providing sensitivity to the top-quark Yukawa coupling. This is the first measurement in ATLAS that aims to obtain this coupling exploiting this approach. The $t\bar{t}$ system is reconstructed in the single-lepton final state, requiring exactly one isolated electron or muon and at least four jets with at least two identified as originating from b-quarks. The measured Yukawa coupling is found to be in good agreement with the Standard Model prediction. An upper limit on the top-quark Yukawa coupling strength of $Y_t < 2.1$ relative to the Standard Model prediction is observed at 95% confidence level, consistent with the expected sensitivity.

Keywords: Top Physics, Hadron-Hadron Scattering, Higgs Physics

ArXiv ePrint: 2509.16039

https://doi.org/10.1007/JHEP01(2026)117

JHEP01(2026)117

Contents

1 Introduction

In the Standard Model (SM), fermions obtain their masses (m_f) via spontaneous symmetry breaking as described by the Englert-Brout-Higgs mechanism [1–6]. The coupling between the Higgs-boson and fermion fields is described by a Yukawa coupling $g_f = \sqrt{2}m_f/v$ where $v = 246.22$ GeV [7] is the vacuum expectation value of the Higgs field.

Since the top-quark mass is heavier than half the mass of the Higgs boson, the top Yukawa coupling (g_t) is the only fermion Yukawa coupling that cannot be measured directly from Higgs boson decays. The most model-independent direct measurement uses the $t\bar{t}H$ process [8–10] where the result depends on the total width of the Higgs boson. Complementary information can be obtained from other processes, such as $gg \to H$ or $H \to \gamma\gamma$ [9, 10] where the top quarks appear in a loop, or from four-top-quark production [11, 12], where off-shell Higgs bosons can be produced. In addition, virtual corrections involving Higgs bosons also have a significant impact on the $t\bar{t}$ production cross-section [13]. The numerically relevant corrections include a Higgs boson exchange between any two top-quark lines. In case the Standard

JHEP01(2026)117

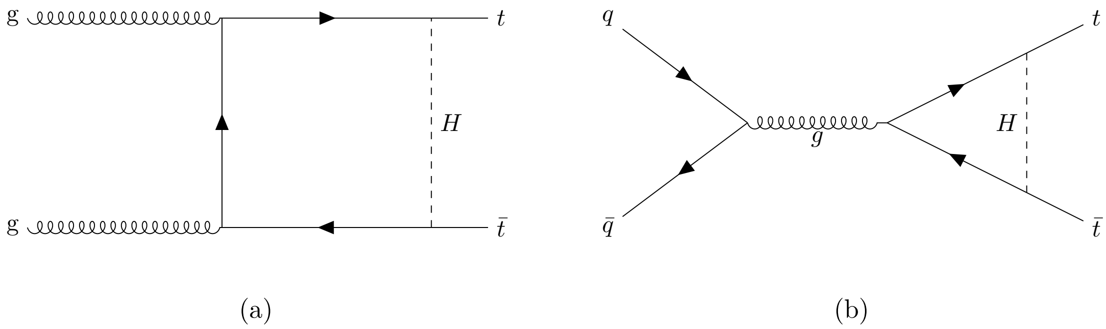

Figure 1. Example Feynman diagrams for (a) gg and (b) $q\bar{q}$ $t\bar{t}$ production with virtual Higgs boson exchange.

Model holds, all measurements result in a coupling strength Y_t $(= g_t/g_t^{\mathrm{SM}})$[1] compatible with unity. However, if physics beyond the SM exists, it could affect each of these measurements differently, making them complementary.

Examples of Feynman diagrams for virtual Higgs-boson corrections to $t\bar{t}$ production are shown in figure 1. The corresponding amplitudes depend on Y_t^2 and are sizeable mainly near the $t\bar{t}$ production threshold, where the top and anti-top quarks have a small relative velocity. The largest sensitivity is therefore expected in this kinematic region. Interfering with the Born level amplitudes, the corrections to the cross-section are also quadratic in Y_t. One can therefore extract Y_t^2 from a measurement of the $t\bar{t}$ production cross-section as a function of the $t\bar{t}$ invariant mass, $m_{t\bar{t}}$. The corrections also depend on the top quark scattering angle in the $t\bar{t}$ rest frame, $\cos\theta^*$, although this dependence is weak in the kinematic region most relevant for the measurement. The method is insensitive to the sign of the Yukawa coupling. Therefore Y_t is always assumed to be $|Y_t|$ in this paper. While the sensitivity to Y_t from virtual corrections is not expected to match that of direct measurements, such as those from $t\bar{t}H$ production [8–10], the approach remains highly valuable. As demonstrated in ref. [14], contributions from new physics, such as a top-philic scalar, can modify the virtual corrections in a way that mimics a deviation in Y_t, potentially affecting indirect and direct extractions differently. Similar models are tested by searches in four-top final states [15] and by searches for new Higgs bosons decaying into $t\bar{t}$ [16].

The CMS Collaboration already performed this analysis in the single lepton channel [17] and in the dilepton channel [18], obtaining observed 95% confidence level upper limits on Y_t of 1.67 and 1.54, respectively.

In this paper, the first ATLAS measurement of Y_t extracted from top-quark pair production is presented. The measurement uses the ATLAS data at $\sqrt{s} = 13$ TeV with an integrated luminosity of 140 fb^{-1}. The single-lepton channel is analysed where the $t\bar{t}$ invariant mass can be fully reconstructed and the background is low. Electroweak (EW) corrections for variable Y_t are calculated in [13, 19, 20] and implemented in HATHOR [21], a program that calculates the $t\bar{t}$ cross-section at parton level in leading-order QCD. They are used to reweight fully-simulated Monte Carlo (MC) events. The weighting is done as a function of the initial-state parton flavour, the generated $m_{t\bar{t}}$ and $\cos\theta^*$. This allows to predict the $m_{t\bar{t}}$

[1] Y_t is identical to the coupling strength modifier κ_t as defined e.g. in refs. [9, 10].

spectra as a function of Y_t. The measured $m_{t\bar{t}}$ spectrum is then fitted in a profile likelihood fit, using these predictions with Y_t^2 as the parameter of interest, together with a set of nuisance parameters representing the systematic uncertainties.

A brief description of the ATLAS detector is provided in section 2, followed by an overview of the data and MC samples in section 3, with section 3.3 describing the electroweak corrections applied in the analysis. Section 4 explains the event reconstruction and selection procedures, including the estimate of the fake-lepton background. The systematic uncertainties are discussed in section 5, and the fit strategy is outlined in section 6. Finally, the results are presented in section 7, with conclusions summarised in section 8.

2 ATLAS detector

The ATLAS detector [22] at the Large Hadron Collider (LHC) [23] covers nearly the entire solid angle around the collision point.[2] It consists of an inner tracking detector surrounded by a thin superconducting solenoid, electromagnetic and hadronic calorimeters, and a muon spectrometer incorporating three large superconducting air-core toroidal magnets.

The inner-detector system (ID) is immersed in a 2 T axial magnetic field and provides charged-particle tracking in the range $|\eta| < 2.5$. The high-granularity silicon pixel detector covers the vertex region and typically provides four measurements per track, the first hit generally being in the insertable B-layer (IBL) installed before Run 2 [24, 25]. It is followed by the SemiConductor Tracker (SCT), which usually provides eight measurements per track. These silicon detectors are complemented by the transition radiation tracker (TRT), which enables radially extended track reconstruction up to $|\eta| = 2.0$. The TRT also provides electron identification information based on the fraction of hits (typically 30 in total) above a higher energy-deposit threshold corresponding to transition radiation.

The calorimeter system covers the pseudorapidity range $|\eta| < 4.9$. Within the region $|\eta| < 3.2$, electromagnetic calorimetry is provided by barrel and endcap high-granularity lead/liquid-argon (LAr) calorimeters, with an additional thin LAr presampler covering $|\eta| < 1.8$ to correct for energy loss in material upstream of the calorimeters. Hadronic calorimetry is provided by the steel/scintillator-tile calorimeter, segmented into three barrel structures within $|\eta| < 1.7$, and two copper/LAr hadronic endcap calorimeters. The solid angle coverage is completed with forward copper/LAr and tungsten/LAr calorimeter modules optimised for electromagnetic and hadronic energy measurements respectively.

The muon spectrometer (MS) comprises separate trigger and high-precision tracking chambers measuring the deflection of muons in a magnetic field generated by the superconducting air-core toroidal magnets. The field integral of the toroids ranges between 2.0 and 6.0 T m across most of the detector. Three layers of precision chambers, each consisting of layers of monitored drift tubes, cover the region $|\eta| < 2.7$, complemented by cathode-strip

[2]ATLAS uses a right-handed coordinate system with its origin at the nominal interaction point (IP) in the centre of the detector and the z-axis along the beam pipe. The x-axis points from the IP to the centre of the LHC ring, and the y-axis points upwards. Polar coordinates (r, ϕ) are used in the transverse plane, ϕ being the azimuthal angle around the z-axis. The pseudorapidity is defined in terms of the polar angle θ as $\eta = -\ln\tan(\theta/2)$ and is equal to the rapidity $y = \frac{1}{2}\ln\left(\frac{E+p_z}{E-p_z}\right)$ in the relativistic limit. Angular distance is measured in units of $\Delta R \equiv \sqrt{(\Delta y)^2 + (\Delta\phi)^2}$.

JHEP01(2026)117

chambers in the forward region, where the background is highest. The muon trigger system covers the range $|\eta| < 2.4$ with resistive-plate chambers in the barrel, and thin-gap chambers in the endcap regions.

The luminosity is measured mainly by the LUCID–2 [26] detector that records Cherenkov light produced in the quartz windows of photomultipliers located close to the beampipe.

Events are selected by the first-level trigger system implemented in custom hardware, followed by selections made by algorithms implemented in software in the high-level trigger [27]. The first-level trigger accepts events from the 40 MHz bunch crossings at a rate below 100 kHz, which the high-level trigger further reduces in order to record complete events to disk at about 1.25 kHz.

A software suite [28] is used in data simulation, in the reconstruction and analysis of real and simulated data, in detector operations, and in the trigger and data acquisition systems of the experiment.

3 Data and simulation samples

Proton-proton (pp) collisions at $\sqrt{s} = 13$ TeV collected in 2015–2018 by the ATLAS experiment are analysed [29]. Only the events where all components of the ATLAS detector were fully functional are selected, resulting in a total dataset corresponding to an integrated luminosity of 140 fb^{-1}. Selected events are required to be triggered by one of the unprescaled single-lepton triggers which are further described in section 4.2.

MC simulated event samples are used to estimate the signal and background contributions containing prompt leptons. Backgrounds containing misidentified or non-prompt leptons stemming e.g. from heavy-flavour decays are determined using data-driven approach as detailed in section 4.4.

The ATLAS simulation infrastructure [30] is used for all the simulation samples, with the detector response simulated using the GEANT [31] framework. For the estimate of several signal modelling uncertainties, a fast simulation, which utilises parametrisations of the hadronic showers in the EM and hadronic calorimeters to speed up the simulation [32], is used. All simulation samples are processed with the same reconstruction software as the data samples.

To account for additional pp interactions from the same or close-by bunch crossings (pile-up), a set of minimum-bias interactions generated with PYTHIA 8.186 [33] using the NNPDF2.3LO parton distribution function (PDF) set [34] with the A3 set of tuned parameters (tune) [35] is superimposed to the hard scattering events. Furthermore, the simulated events are reweighted according to the number of additional pp interactions per bunch crossing to match the pile-up conditions of each dataset corresponding to the 2015–2018 years of data-taking. Corrections are applied to simulated events to improve agreement between the data and the simulation samples in the object identifications, efficiencies, energy scales, and energy resolutions, as described in section 4.1.

Heavy-flavour decays are modelled with the EVTGEN program [36] in all parton shower generators, with the exception of the SHERPA [37] generator.

JHEP01(2026)117

3.1 Signal modelling

The nominal signal $t\bar{t}$ MC sample is simulated using POWHEG BOX-v2 [38–40] which is based on next-to-leading-order (NLO) QCD matrix element (ME) calculations. The calculation for the ME uses the NNPDF3.0NLO PDF set [41] with a top-quark mass (m_t) of 172.5 GeV. The h_{damp} parameter that controls the emission of the first gluon is set to $1.5m_t$. The renormalisation (μ_{r}) and factorisation (μ_{f}) scales are defined by the functional form $\sqrt{m_t^2 + p_{\mathrm{T},t}^2}$, where $p_{\mathrm{T},t}$ is the transverse momentum of the top quark. The ME generator is interfaced with PYTHIA 8.230 [42] which simulates parton shower (PS), fragmentation, hadronisation, and the underlying event. The A14 tune [43] together with NNPDF2.3LO PDF set is applied for PYTHIA 8 showering. The $p_{\mathrm{T}}^{\mathrm{hard}}$ parameter which impacts the matching of the ME to PS, is set to zero [44].

A number of signal modelling uncertainties are estimated using alternative MC samples. To compare the effect of different PS and hadronisation modelling, a sample produced with POWHEG BOX-v2 interfaced with HERWIG 7.2.1 [45, 46] with the MMHT2014LO PDF set [47] and the default set of tuned parameters, is used. The POWHEG settings are the same as in the nominal sample. For the estimate of the h_{damp} uncertainty, an alternative sample with the same generator and settings as the nominal $t\bar{t}$ sample and the h_{damp} parameter doubled to $3m_t$, is used. Similarly, alternative samples based on the nominal sample with m_t varied to 172 GeV and 173 GeV, respectively, are used to estimate the impact of the assumption on m_t on the analysis. Finally, to estimate the uncertainty in the ME-to-PS matching, a MC sample produced with the same generator and the same settings as the default $t\bar{t}$ sample is used, except for the $p_{\mathrm{T}}^{\mathrm{hard}}$ parameter setting, which is set to $p_{\mathrm{T}}^{\mathrm{hard}} = 1$ [44]. The $t\bar{t}$ production threshold is potentially sensitive to the modelling of off-shell effects and top-quark decay. To estimate the uncertainty in the modelling of these effects, an alternative sample based on the nominal $t\bar{t}$ sample, but with the MADSPIN generator interfaced to POWHEG BOX-v2 to simulate the top-quark decay [48, 49], is used.

All $t\bar{t}$ MC samples are normalised to next-to-next-to-leading-order (NNLO) cross-section including the resummation of soft gluon emissions at next-to-next-to-leading-logarithmic (NNLL) accuracy using TOP++2.0 [50]. The resulting cross-section for the $t\bar{t}$ process is $\sigma_{t\bar{t}} = 834^{+21}_{-30}(\mathrm{scale}) \pm 21(\mathrm{PDF} + \alpha_S)$ pb for $m_t = 172.5$ GeV [51–56].

Additionally, a dedicated fixed-order NNLO QCD prediction [57, 58] is used to define an uncertainty due to missing higher-order corrections. It is calculated using the MATRIX tool [59–64], using the NNPDF3.0NNLO PDF set [41] and assuming $m_t = 172.5$ GeV. The functional form of the μ_{r} and μ_{f} scales is set to $H_{\mathrm{T}}/4$, where $H_{\mathrm{T}} = \sqrt{m_t^2 + p_{\mathrm{T},t}^2} + \sqrt{m_t^2 + p_{\mathrm{T},\bar{t}}^2}$, based on recommendations in ref. [65]. The prediction is calculated in terms of a two-dimensional distribution of $m_{t\bar{t}}$ and the cosine of the angle between the top-quark momentum boosted to the $t\bar{t}$ rest-frame and the momentum of the $t\bar{t}$ system in the laboratory frame. Subsequently, the nominal $t\bar{t}$ MC sample is reweighted using this prediction to create a systematically varied alternative sample.

3.2 Background modelling

In the $t\bar{t}$ threshold region, the formation of a colour-singlet $t\bar{t}$ quasi-bound state, commonly referred to as the *toponium*, is expected, consistent with the recent CMS [66] observation indicating an excess in the $t\bar{t}$ threshold region. The toponium contribution is described using a simplified model [67, 68], as a pseudo-scalar s-channel resonance, since the dominant contribution to the $gg \to t\bar{t}$ colour-singlet quasi-bound state comes from pseudo-scalar $J = 0$ states [69]. The width of the resonance is set to 2.8 GeV and the mass of the resonance to 343 GeV, assuming that the toponium quasi-bound state has twice the mass of the top quark minus the binding energy of approximately 2 GeV [69, 70]. The toponium events are simulated using MadGraph 3.5.5 with the NNPDF3.0nlo PDF set, interfaced to Pythia 8.3 [71] for PS and hadronisation modelling. At present, the impact of electroweak corrections on the toponium is unknown and thus neglected. Therefore, the toponium contribution is considered as a background process. It is normalised to a non-relativistic perturbative QCD prediction of 6.43 pb [67, 70].

Single-top quark processes are split into s-channel, t-channel and tW-channel contributions. They are simulated using the same setup as the nominal $t\bar{t}$ sample, using the five-flavour scheme in the PDF set, with the exception of the t-channel process, which is generated using the four-flavour scheme. The overlap between $t\bar{t}$ and single-top Wt final states is removed using the diagram removal (DR) technique [72] and an additional sample using diagram subtraction (DS) [72, 73] is used for the estimate of the corresponding modelling uncertainty. The single-top samples are normalised to NNLO QCD predictions for the s- and t-channels [74, 75] and to approximate N^{3}LO QCD prediction for the tW channel [76]

Several background processes are simulated using different versions of the Sherpa [77] generator, with the details outlined below. Sherpa includes both the ME, PS and hadronisation modelling. The matrix elements are computed using Comix [78] and OpenLoops [61]. The NNPDF3.0nlo PDF set is used with a dedicated tune provided by the Sherpa authors. The ME is merged with the Sherpa PS using the MEPS@NLO prescription [79].

Events with a Z or W boson in association with additional jets are simulated with the Sherpa 2.2.11 generator. The matrix elements for up to two additional partons are calculated at NLO QCD precision, and at LO QCD for up to four additional partons. The samples are normalised to the NNLO QCD prediction [80, 81].

Diboson ($WW/WZ/ZZ$) samples are simulated using Sherpa 2.2.1. The matrix elements for up to one additional parton are calculated at NLO QCD precision, and at LO QCD accuracy for up to three additional partons. The samples are normalised to the NLO QCD theoretical cross-sections [82].

A minor contribution to the total background originates from boson-associated $t\bar{t}$ production. The production of $t\bar{t}Z$ events is modelled using the MadGraph5_aMC@NLO 2.3.3 [83] generator at NLO with the NNPDF3.0nlo PDF set. The events are interfaced to Pythia 8.210 using the A14 tune and the NNPDF2.3lo PDF set. The $t\bar{t}W$ process is simulated using Sherpa 2.2.10 [77]. The matrix element is calculated at NLO QCD for up to one additional parton and up to two additional partons at LO QCD. The production of $t\bar{t}H$ events is modelled using the Powheg Box v2 [84] generator at NLO with the NNPDF3.0nlo PDF set, interfaced to Pythia 8.230 using the A14 tune and the NNPDF2.3lo PDF set. The samples corresponding to all three processes are normalised to the NLO QCD+EW predictions [85].

JHEP01(2026)117

3.3 Electroweak corrections

To obtain the signal samples for different Y_t values, a reweighting technique is used on the nominal $t\bar{t}$ sample, which is based on a leading-order calculation for the full electroweak corrections where Y_t is a free parameter.

The electroweak corrections with variable Y_t as calculated in [13, 19, 20] and implemented in HATHOR 2.1-b3 [21] are used. The program evaluates the leading-order electroweak corrections to the Born level $q\bar{q} \to t\bar{t}$ and $gg \to t\bar{t}$ cross-sections as a function of $m_{t\bar{t}}$ and $\cos\theta^*$ assuming stable top quarks. More recent predictions for the electroweak corrections exist, including additional amplitudes with the s-channel Higgs boson exchange diagrams [14], which are not considered in the predictions obtained from HATHOR. These amplitudes have a sizeable impact on CP-odd extensions of the Yukawa interaction. However, for the measurement presented here, which assumes a CP-even Y_t, their impact is negligible [14]. The impact of a modified Y_t on the $t\bar{t}$ production cross-section is evaluated in two steps. HATHOR predictions as functions of $m_{t\bar{t}}$ and $\cos\theta^*$ are first parameterised with smooth functions. These are then used to compute event weights, defined as the ratio of predictions for a given Y_t to those without EW corrections applied. These weights are applied to the events generated with the nominal POWHEG+PYTHIA setup. The weights depend on the parton-level $m_{t\bar{t}}$ and $\cos\theta^*$, and initial-state parton flavour. This corresponds to the multiplicative approach combining electroweak and QCD corrections. At $\sqrt{s} = 13$ TeV, about 2% of the POWHEG events originate from a qg or $\bar{q}g$ initial state. For them the EW corrections corresponding to the gg initial state are used for reweighting. This is a valid approach as in the region near the threshold, where the sensitivity is the largest, the correction depends very little on the initial state. The top-quark mass is set to $m_t = 172.5$ GeV, consistent with the signal Monte Carlo samples used in the analysis. The weights are calculated as a function of Y_t. For gg initial states, in all Feynman diagrams containing virtual Higgs boson corrections, the Higgs boson is connected to two top-quark lines. For $q\bar{q}$ initial states, the same is true for the numerically dominant diagrams. For this reason, the corrections are proportional to Y_t^2. The Y_t-dependent electroweak correction as a function of $m_{t\bar{t}}$ are shown in figure 2 for the quark-induced as well as for the gluon-induced processes.

4 Event reconstruction and selection

4.1 Object definitions

Events are required to have at least one reconstructed pp interaction vertex with a minimum of two associated tracks with transverse momenta $p_{\mathrm{T}} > 0.5$ GeV. The primary vertex is defined as the vertex with the highest sum of squared transverse momenta of associated tracks [86].

Electron candidates are reconstructed from energy deposits in the electromagnetic calorimeter matched to a track in the ID [87]. The track is required to be matched to the primary vertex, where the track longitudinal impact parameter z_0, must satisfy $|z_0 \sin\theta| <$ 0.5 mm and the transverse impact parameter d_0 and its uncertainty $\sigma(d_0)$ must satisfy $|d_0/\sigma(d_0)| < 5$. Electron candidates are required to be within $|\eta| < 2.47$, excluding the transition region between the barrel and the end-cap calorimeters, $1.37 < |\eta| < 1.52$. They

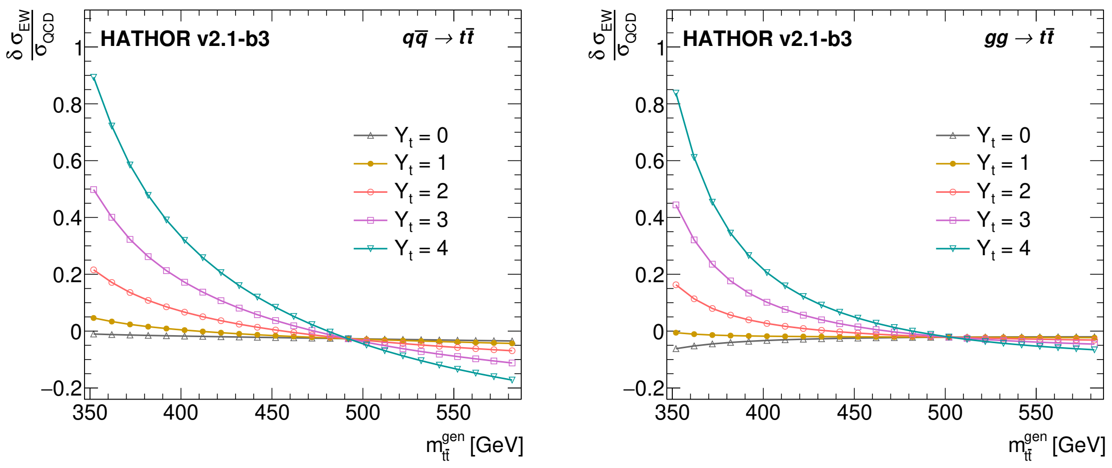

(a)

(b)

Figure 2. Ratio of the electroweak corrections ($\delta\sigma_{\text{EW}} = \sigma_{\text{QCD+EW}} - \sigma_{\text{QCD}}$) over the leading-order QCD cross-section (σ_{QCD}) at parton level, as a function of $m_{t\bar{t}}^{\text{gen}}$, the $t\bar{t}$ mass calculated directly from the top quark and top antiquark four-momenta at generator level, for different Y_t values from (a) quark-antiquark annihilation and (b) gluon-gluon fusion processes, calculated with HATHOR 2.1-b3 [21].

must satisfy $p_{\text{T}} > 25$ GeV and the *Tight* likelihood identification criteria and *Tight* isolation criteria [87].

Muon candidates are reconstructed by associating tracks in the ID with tracks or track segments in the MS [88], refined through a global fit that uses hits from both subdetectors [89]. The track longitudinal and transverse impact parameters must satisfy the requirements $|z_0 \sin\theta| < 0.5$ mm and $|d_0/\sigma(d_0)| < 3$, respectively. Muon candidates must satisfy $p_{\text{T}} > 25$ GeV, $|\eta| < 2.5$ and the *Medium* identification and *Tight* isolation criteria [88].

Jets are reconstructed from particle-flow objects [90, 91] using the anti-k_t algorithm [92, 93] with a jet radius parameter $R = 0.4$. The jet energy scale (JES) is calibrated using both data and simulation, as detailed in Reference [91]. Additionally, the jet energy resolution (JER) in simulation is corrected to match the resolution observed in data [91]. Jets are required to satisfy $p_{\text{T}} > 25$ GeV and $|\eta| < 2.5$. To suppress jets originating from pile-up interactions, the *jet vertex tagger* (JVT) multivariate likelihood [94] discriminant, using track-based variables, is applied to jets satisfying $p_{\text{T}} < 60$ GeV and $|\eta| < 2.4$, ensuring that the selected jets are matched to the primary vertex. Jets originating from B-hadrons (b-jets) are identified using the DL1r deep neural network algorithm [95], using a working point corresponding to a 77% efficiency to correctly tag a b-jet in $t\bar{t}$ events, providing rejection factors of approximately 6 and 134 for charm and light-flavoured jets, respectively. Correction factors are applied to the simulated events to compensate for differences between data and simulation in the b-tagging efficiency for b-, c- and light-flavoured jets.

The missing transverse energy, $E_{\text{T}}^{\text{miss}}$, is defined as the magnitude of the negative vectorial sum of the transverse momenta of all calibrated electrons, muons and jets in the event. Tracks that are not associated with any of the physics objects but originate from the primary vertex are taken into account as a soft term [96].

To avoid the double-counting of the same energy deposits in multiple objects due to reconstruction ambiguities, an overlap removal procedure is applied. First, jets within $\Delta R < 0.2$ of an electron are removed. Electrons within $\Delta R < 0.4$ of a jet are removed. Jets with less than three ID tracks within $\Delta R < 0.2$ of a muon are removed to avoid rejecting high-energy muons affected by calorimeter energy loss. Finally, muons within $\Delta R < 0.4$ of remaining jets are removed.

4.2 Event selection

A number of event selection criteria are imposed to select events with a topology expected for $t\bar{t}$ production with a single prompt lepton in the final state.

The candidate events are required to have fired one of the single-electron or single-muon triggers [97, 98] and to have at least one trigger-matched electron or muon with $p_{\mathrm{T}} > 27$ GeV, ensuring that the employed triggers are fully efficient. For the 2015 data-taking period, a leading-lepton cut of $p_{\mathrm{T}} > 25$ GeV is applied due to lower trigger thresholds. Events with additional electrons or muons with $p_{\mathrm{T}} > 25$ GeV are rejected. At least four jets with $p_{\mathrm{T}} > 25$ GeV are required, out of which at least two of the jets are required to be b-tagged.

The candidate events are further categorised based on the lepton flavour into two signal regions (SRs): e+jets SR and μ+jets SR. To suppress background events containing a non-prompt or a misidentified lepton, the following selection criteria are applied. Events in the e+jets SR are required to satisfy $E_{\mathrm{T}}^{\mathrm{miss}} > 30$ GeV and the reconstructed W boson transverse mass[3] $m_W^{\mathrm{T}} > 30$ GeV. Events in the μ+jets SR are required to satisfy $E_{\mathrm{T}}^{\mathrm{miss}} + m_W^{\mathrm{T}} > 60$ GeV. The split of events into separate e+jets and μ+jets SRs is performed to accurately capture the impact and the correlations of systematic uncertainties impacting leptons, jets and signal modelling. Due to the different event selections, these sources of uncertainty can impact the two SRs differently.

Additionally, for the non-prompt and misidentified leptons background estimate, two control regions (CRs), named fake-e CR and fake-μ CR, are defined by inverting the $E_{\mathrm{T}}^{\mathrm{miss}}$ and m_W^{T} requirements of the e+jets SR and μ+jets SR, respectively.

Finally, to suppress contribution from poorly reconstructed $t\bar{t}$ events in SRs, additional selection criteria on event kinematics are imposed in the $t\bar{t}$ reconstruction, described in the next section.

4.3 $t\bar{t}$ reconstruction

As mentioned in section 1, the sensitivity to Y_t is enhanced in the $m_{t\bar{t}}$ distribution close to the $t\bar{t}$ production threshold. Hence, in order to measure the $t\bar{t}$ invariant mass, the four-momenta of the top and the anti-top quarks are reconstructed from the event information using a dedicated algorithm which aims to find the correct assignment of reconstructed objects to the decay products of the two top quarks. If the event contains more than two b-jets, the two leading-p_{T} b-jets are considered in the reconstruction. The hadronically decaying top quark is reconstructed first. If the event contains only two jets in addition to the two b-jets, they are used to reconstruct the hadronic W boson candidate. If there are three or more additional jets, the three with the highest p_{T} are selected, and the pair with an invariant mass

[3] $m_W^{\mathrm{T}} = \sqrt{(E_{\mathrm{T}}^{\mathrm{miss}} + E_{\mathrm{T},\ell})^2 - (\vec{p}_{\mathrm{T}}^{\,\mathrm{miss}} + \vec{p}_{\mathrm{T},\ell})^2}$.

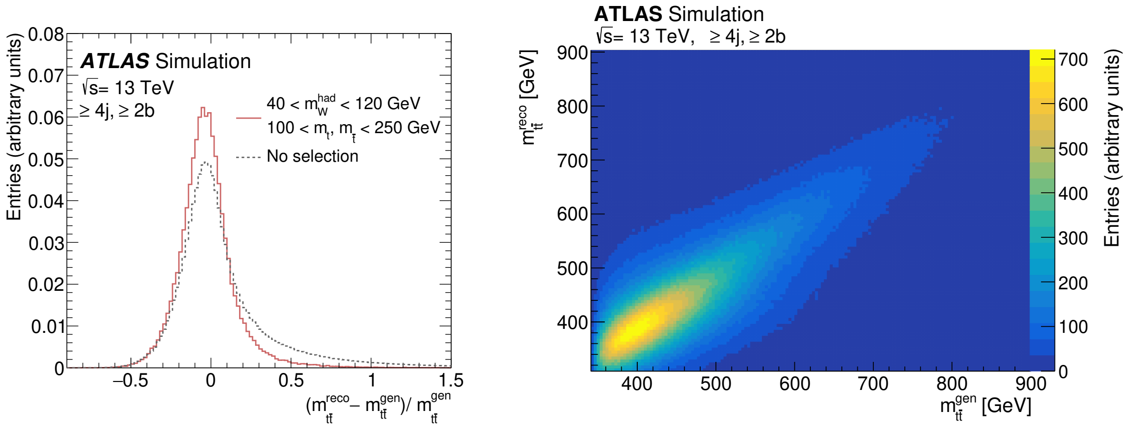

(a) (b)

Figure 3. Reconstructed $m_{t\bar{t}}$ resolution and the correlation of the reconstructed $m_{t\bar{t}}$ with the generator level $m_{t\bar{t}}$ distribution. (a) The $m_{t\bar{t}}$ resolution distributions after the m_t and m_W^{had} requirements, compared with the case without these selections. (b) The reconstructed $m_{t\bar{t}}$ after applying the selection of $m_W^{\text{had}} \in [40, 120]$ GeV and $m_t \in [100, 250]$ GeV, plotted against the generated $m_{t\bar{t}}$.

closest to the W boson mass is used for the hadronic W boson reconstruction. The hadronic W candidate is combined with the b-jet yielding the mass closest to the top-quark mass to reconstruct the hadronically decaying top-quark candidate. Thereafter, the leptonically decaying top quark is reconstructed from the kinematics of the lepton, the leftover b-jet and the missing transverse energy, which represents the only available information about the neutrino kinematics. To obtain the z-component of the neutrino momentum, a constraint on the W boson mass is exploited. Assuming energy-momentum conservation, a quadratic equation is obtained as a function of the neutrino p_z. If two real solutions are obtained, the one yielding an invariant mass of the leptonically decaying top quark closest to the top-quark mass is considered. If no real solutions are obtained, the magnitude and ϕ of E_T^{miss} are altered in small steps until a solution is obtained.

The resolution of the reconstructed mass, defined as the ratio of the difference between the reconstructed ($m_{t\bar{t}}^{\text{reco}}$) and the generated ($m_{t\bar{t}}^{\text{gen}}$) $t\bar{t}$ masses,[4] over the generated $t\bar{t}$ mass value, is shown by a dashed line in figure 3(a). The distribution is centred around zero but exhibits a positive tail, making the average reconstructed $m_{t\bar{t}}$ larger than the generated value. The presence of this tail may be partially attributed to incorrect jet assignments. A detailed jet-to-parton association study is performed to mitigate the selection of such events, resulting in requirements on the hadronic W boson mass (m_W^{had}) and on the hadronic and leptonic top quark masses. After selecting the events with $m_W^{\text{had}} \in [40, 120]$ GeV and $m_t \in [100, 250]$ GeV, an improvement in the resolution can be seen, as shown by the distribution with a solid line in figure 3(a). The selection does not bias the $m_{t\bar{t}}$ distribution in the threshold region and consequently does not cause a bias in the Y_t extraction. Figure 3(b) shows the correlation

[4] $m_{t\bar{t}}^{\text{gen}}$ represents the $t\bar{t}$ mass calculated directly from the top quark and top antiquark four-momenta at generator level.

JHEP01(2026)117

of the resultant reconstructed $m_{t\bar{t}}$ with the generated $m_{t\bar{t}}$ for events satisfying the specified requirements on $m_W^{\rm had}$ and m_t.

4.4 Non-prompt and fake leptons background

The background originating from events resembling the signal topology with either a non-prompt or misidentified lepton (referred to as *fake* lepton) is poorly modelled in the simulation. Therefore, the fake-lepton contribution is estimated with the data-driven *matrix method* [99], using events with relaxed (*loose*) lepton selection criteria and utilising measurements of efficiencies of the *loose* leptons to satisfy baseline (*tight*) selection criteria. The efficiencies are binned in lepton $p_{\rm T}$, where the prompt lepton efficiencies are determined from the nominal $t\bar{t}$ simulation in the SRs. The fake-lepton efficiencies are determined from data in the fake CRs, where the contribution of prompt leptons, estimated from simulation, is subtracted from data. For both *loose* electrons [87] and *loose* muons [88], the isolation criterion is dropped. Additionally, *loose* electrons are required to satisfy a relaxed *LooseAndBLayerLH* identification [87], while *loose* muons have a relaxed $|d_0/\sigma(d_0)| < 7$ criterion.

Due to the $\geq 2b$-jet requirement, which leads to a very high signal purity, the fake-lepton background is very small and thus there is a substantial contribution of prompt leptons in the fake CRs. Therefore, any mis-modelling of the prompt lepton contribution can have a significant impact on the fake-lepton efficiency. In particular, the $t\bar{t}$ simulation is known to mis-model the lepton $p_{\rm T}$ distribution. This is mitigated, only for the purpose of the fake-lepton estimate, by reweighting the $t\bar{t}$ lepton $p_{\rm T}$ based on the background-subtracted data in the SRs, ignoring the fake-lepton contribution, and applying the reweighting to the lepton $p_{\rm T}$ distribution in the fake CRs. A closure test is performed, where the $t\bar{t}$ lepton $p_{\rm T}$ reweighting is repeated after including the final fake-lepton estimate. No significant change in the prompt lepton contribution in the fake lepton CRs is observed.

Furthermore, a free correction factor (CF) to the prompt lepton efficiency is introduced in the fake CRs to account for differences between the modelling of loose and tight prompt leptons. The value of the CF is determined such that the estimated fake-lepton $m_W^{\rm T}$ distribution is flat around the W boson mass in the SRs, indicating that the prompt background was subtracted correctly. The central value of the CF is close to unity and a systematic variation on the CF is considered, resulting in a variation of up to 20% on the fake-lepton $m_{t\bar{t}}$ distribution.

The resulting fake-lepton background constitutes a very small fraction of approximately 0.7% ± 0.3% of the total expected signal and background contribution in the SRs.

5 Systematic uncertainties

The measurement is impacted by systematic uncertainties, ranging from experimental uncertainties, signal and background modelling uncertainties and uncertainties due to the finite amount of MC events. For systematic uncertainties defined by both “up” and “down” variations, a symmetrised uncertainty is obtained by taking the arithmetic average of the magnitudes of the two variations, unless otherwise specified. For one-sided systematic uncertainties, the “up” uncertainty is mirrored to obtain the “down” variation. The systematic variations are smoothed to reduce the impact of statistical fluctuations due to finite amount of generated Monte Carlo sample events.

JHEP01(2026)117

5.1 Experimental uncertainties

A number of experimental uncertainties are considered which are related to object reconstruction, pile-up modelling and luminosity. They are applied to all the processes other than the non-prompt and fake-lepton background.

The uncertainty in the integrated luminosity is 0.83% [100]. Additionally, to match the pile-up distribution of simulation to data, a rescaling of the average number of interaction per bunch crossing is applied to the simulation. An uncertainty in the rescaling is propagated by varying the corresponding pile-up reweighting factors.

For electrons and muons, the uncertainties in the trigger, identification, isolation and reconstruction efficiencies are included, which are derived from studies using $Z \to ee$ [87, 97] and $Z \to \mu\mu$ events [88, 98], respectively. Additionally, uncertainties in the electron energy scale and muon momentum scale and their resolutions are evaluated using dedicated measurements in data [87, 101].

Systematic uncertainties in JES and JER are evaluated using a series of simulation-based techniques and in situ measurements [91, 102]. These include uncertainty components related to the jet flavour composition, η-intercalibration, punch-through, single-particle response, calorimeter response to different jet flavours and pile-up effects. They are comprised of 30 uncorrelated JES components and 13 uncorrelated JER components. Additionally, an uncertainty in the calibration of the efficiency of the JVT is evaluated by varying the associated correction factor [94]. The "up" and "down" JER variations are not symmetrised due to a significantly asymmetrical impact on the fitted $m_{t\bar{t}}$ distribution.

Uncertainties in the calibrations of the b-tagging algorithm in data are propagated by varying the tagging efficiency correction factors [103–105]. These include nine, four and four components for the b, c and light-flavoured jet calibrations, respectively, and two components related to the extrapolation to high-p_{T} jets.

The uncertainties related to the energy scale and resolution of leptons and jets are propagated to $E_{\mathrm{T}}^{\mathrm{miss}}$. Additional uncertainties in $E_{\mathrm{T}}^{\mathrm{miss}}$ arise from momentum scale and resolution uncertainties of the track-based soft term [96].

5.2 Signal modelling uncertainties

A number of signal modelling uncertainties are considered. A normalisation uncertainty of $^{+3.6}_{-4.5}\%$ on the $t\bar{t}$ process is assigned based on the theory uncertainty of the NNLO+NNLL QCD prediction described in section 3.1. Uncertainties related to the QCD scale variations in the ME are estimated by varying the μ_{r} and μ_{f} scales in the ME calculation independently by factors 2 and 0.5. For the uncertainty in the amount of initial-state radiation (ISR), the first component is estimated by changing α_S^{ISR} via the VAR3C variation of the PYTHIA A14 tune. The second component of the ISR uncertainty is estimated by varying the h_{damp} parameter from $1.5 \times m_t$ to $3 \times m_t$. The uncertainty related to the amount of final-state radiation (FSR) is estimated by varying the μ_{r} scale of α_S^{FSR} in the parton shower by factors 2 and 0.5, respectively. The uncertainty associated with the matching of the matrix element to the parton shower is estimated by varying the $p_{\mathrm{T}}^{\mathrm{hard}}$ parameter in PYTHIA [44]. The uncertainties in the parton shower and hadronisation model are estimated by comparing the sample generated with POWHEG+HERWIG 7.2.1 [46] with the nominal $t\bar{t}$ sample. The

JHEP01(2026)117

corresponding variation is further decomposed into a variation for events with exactly four jets and a variation for events with five or more jets, to reduce strong constraints observed otherwise. A set of 30 eigenvariations in the PDF4LHC15 prescription [106] are considered to estimate the uncertainties in the choice of the PDF set. The $m_{t\bar{t}}$ threshold region is potentially sensitive to uncertainties related to the top-quark mass and decay modelling. The uncertainty in the top-quark mass is propagated by varying its value in the MC simulation by ± 0.5 GeV. The uncertainty in the modelling of the top-quark decay and off-shell effects is estimated by comparing the nominal POWHEG+PYTHIA $t\bar{t}$ sample with a $t\bar{t}$ sample reweighted at parton-level to the POWHEG+MADSPIN+PYTHIA sample in top-quark and top-antiquark mass observables. The uncertainty due to missing higher-order corrections in the ME is estimated by comparing a sample reweighted by a dedicated NNLO QCD prediction, described in section 3.1, with the nominal $t\bar{t}$ sample.

Finally, the application of the EW corrections to the $t\bar{t}$ sample has an associated ambiguity, whether the correction is applied in a multiplicative or additive approach on top of the NLO QCD corrections. Since the QCD corrections are dominantly collinear while the electroweak corrections occur at a much higher scale, the multiplicative approach is considered more accurate. This is particularly true for $t\bar{t}$ production where, due to the large top-quark mass, QCD radiation mostly originates from the initial state, while electroweak corrections almost entirely affect the final state [13]. Therefore, the multiplicative approach is used consistently and the additive approach is evaluated in a simplified way. In the additive approach, the electroweak corrections should only be applied to the Born-level QCD diagrams. This is technically not possible in POWHEG, due to the additional radiation in the ME and because of the interplay between the ME and PS matching. Instead, an approximation is made, rescaling the EW corrections by the ratio of the NLO QCD to the Born cross-section, taken from [70], which corresponds to a factor 0.75 almost independent of $m_{t\bar{t}}$. The difference between the EW corrections in the multiplicative and the additive approach depends on the Y_t value. A complete treatment of this uncertainty would require the introduction of a nuisance parameter that is dependent on the observable of interest. Instead, the uncertainty is defined assuming the SM prediction of $Y_t = 1$. This assumption is deemed reasonable and the resulting uncertainty conservative, given that for this analysis the multiplicative approach is better motivated than the additive approach. For $Y_t = 1$, this uncertainty is smaller than 1%, and the impact on the final result is sub-dominant.

5.3 Background modelling uncertainties

The event selection in the analysis ensures a very low background contamination, with an expected signal purity of 93.5%. Therefore, background modelling uncertainties play a sub-dominant role.

The single-top quark background is the largest background in the analysis, with the tW-channel contributing approximately 2% to the total expected signal and background yield. The normalisation uncertainties considered correspond to the approximate NNLO inclusive cross-section uncertainties of 1.9% for the t-channel [74] and 3.8% for the s-channel [75] production. A 3.6% normalisation uncertainty is assigned to the tW process, corresponding to the approximate N^{3}LO inclusive cross-section [76]. The uncertainties in the amount of ISR and FSR in the single-top quark processes are taken into account using the same variations as for the $t\bar{t}$ process, but treated as uncorrelated with respect to it. These include independent variations of the μ_r and μ_f scales in the ME by a factor 0.5 and 2. Another component includes changing the PYTHIA A14 tune settings to the VAR3C eigentune [43]. The uncertainty in the amount of final-state radiation is estimated by varying the μ_r scale of the parton-shower emissions by factors 2 and 0.5. Additionally, the uncertainty in the treatment of the interference and overlap between tW production and $t\bar{t}$ production is estimated by comparing the tW MC sample using DR scheme with MC sample using the DS scheme instead [72, 73].

For the W+jets production, a normalisation uncertainty of 5% is considered, based on the NNLO QCD cross-section predictions from MATRIX [80]. An additional uncertainty is evaluated by simultaneously varying the μ_r and μ_f scales in the ME by a factor of 0.5 and 2, respectively [107]. The factor 0.5 and 2 variations are not symmetrised due to a significantly asymmetrical impact on the $m_{t\bar{t}}$ distribution.

The uncertainties in the toponium process modelling include a conservative 100% normalisation uncertainty and uncertainties arising from the independent variations of factor 2 and 0.5 of μ_r and μ_f scales in the ME. However, since no information about the angular correlations of decay products is used to exploit the expected pseudo-scalar nature of the toponium, no significant sensitivity to this process is expected.

For the fake-lepton background, a normalisation uncertainty of 50% is considered. Additional uncertainties include a variation of the prompt lepton efficiency CF introduced in section 4.4 and per-bin statistical uncertainties.

Finally, a normalisation uncertainty of 50% is considered for each process of the additional sub-dominant backgrounds including Z+jets, dibosons and $t\bar{t}X$ $(X = Z, W, H)$.

6 Fit strategy

Weights derived from HATHOR are used to produce $m_{t\bar{t}}$ templates for various values of Y_t. A profile likelihood template fit using the TREXFITTER tool is performed, taking these templates into account using a morphing method [108, 109]. Systematic uncertainties are included in the likelihood as nuisance parameters (NPs) with Gaussian constraints. The statistical uncertainty in the signal and background predictions is accounted for by adding a NP for each bin, assuming a Poisson constraint [108].

As explained in section 3.3, the dependence of the EW corrections on Y_t is exactly quadratic. Hence, Y_t^2 is used as the parameter of interest (POI) in the fit, instead of Y_t. The resulting linear dependence of the templates on the POI simplifies the fit and avoids issues with highly non-parabolic likelihood. In the morphing approach used, a normalisation parameter is added to the nominal ($Y_t^2 = 1$) template for each bin, which is parametrised by a linear function of Y_t^2. The per-bin linear function parametrisations are determined from the $m_{t\bar{t}}$ histograms for multiple points in Y_t^2 space, obtaining a continuous linear interpolation in Y_t^2.

The analysis is performed separately in the electron and muon channels, using their respective histogram templates for different Y_t^2 values. A split into regions with exactly 4 jets and ≥ 5 jets was investigated; however, due to strong constraints of signal modelling uncertainties with anti-correlations across the two regions, this approach was rejected. Figure 4 shows the corresponding $t\bar{t}$ signal templates used in the fit. In addition to the templates

JHEP01(2026)117

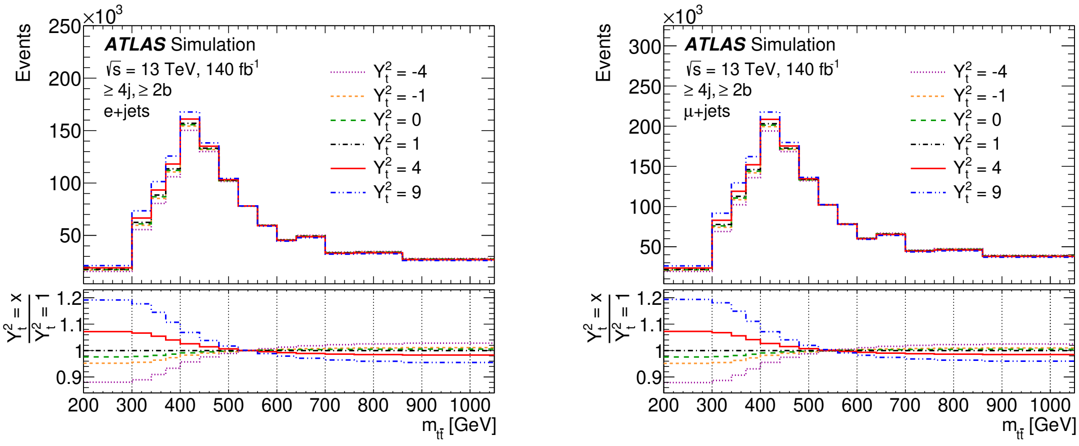

(a) (b)

Figure 4. Reconstructed $m_{t\bar{t}}$ distributions corresponding to the various Y_t^2 templates used in the fit for (a) the electron and (b) the muon channel. The lower panel displays the ratio of the yields for each Y_t^2 template relative to the $Y_t^2 = 1$ template. The negative Y_t^2 templates are unphysical and are used only to improve the fit stability.

corresponding to $Y_t^2 = 0, 1, 4, 9$, histograms corresponding to negative Y_t^2 values are also considered. These non-physical negative Y_t^2 templates are obtained by extrapolating the linear dependence of the electroweak corrections on Y_t^2 to negative values. These templates are introduced in the fit in order to produce a stable fit minimisation with a continuous likelihood function for the situation where the -1σ uncertainty in the fitted Y_t^2 result goes further below zero.

To carefully consider the Y_t-sensitive region, the fit employs an optimised binning strategy. The fitted $m_{t\bar{t}}$ distribution consists of 14 bins in total per channel. Two bins cover the area below the $t\bar{t}$ production threshold. The binning is made finer for $m_{t\bar{t}}$ near the $t\bar{t}$ threshold to preserve Y_t^2 sensitivity. As no steep shape dependence on Y_t^2 is observed in the tail of the $m_{t\bar{t}}$ distribution, and to avoid artificial nuisance parameter constraints in the fit due to a large number of bins, away from the threshold, a wider binning scheme is adopted, with the $m_{t\bar{t}}$ restricted to be below 1050 GeV. Cross-checks are performed to test the fit dependence on the $m_{t\bar{t}}$ range by reducing the maximum $m_{t\bar{t}}$ to 700 GeV and to 500 GeV. No dependence on the extracted central value of Y_t^2 is observed. The sensitivity to Y_t^2 is slightly reduced with the decreased $m_{t\bar{t}}$ range. Extending the fit range up to 1050 GeV leads to a reduction of post-fit correlations of Y_t^2 with signal modelling uncertainties, by providing additional information about their shape and acceptance effects.

7 Results

A comparison of the reconstructed $m_{t\bar{t}}$ distribution for the data to the total prediction before and after the combined fit is shown in figure 5 for the e+jets and μ+jets SRs. The value of Y_t^2 is extracted by performing a profile-likelihood fit to the data as explained in section 6. The expected and observed negative log-likelihood distributions are shown in

JHEP01(2026)117

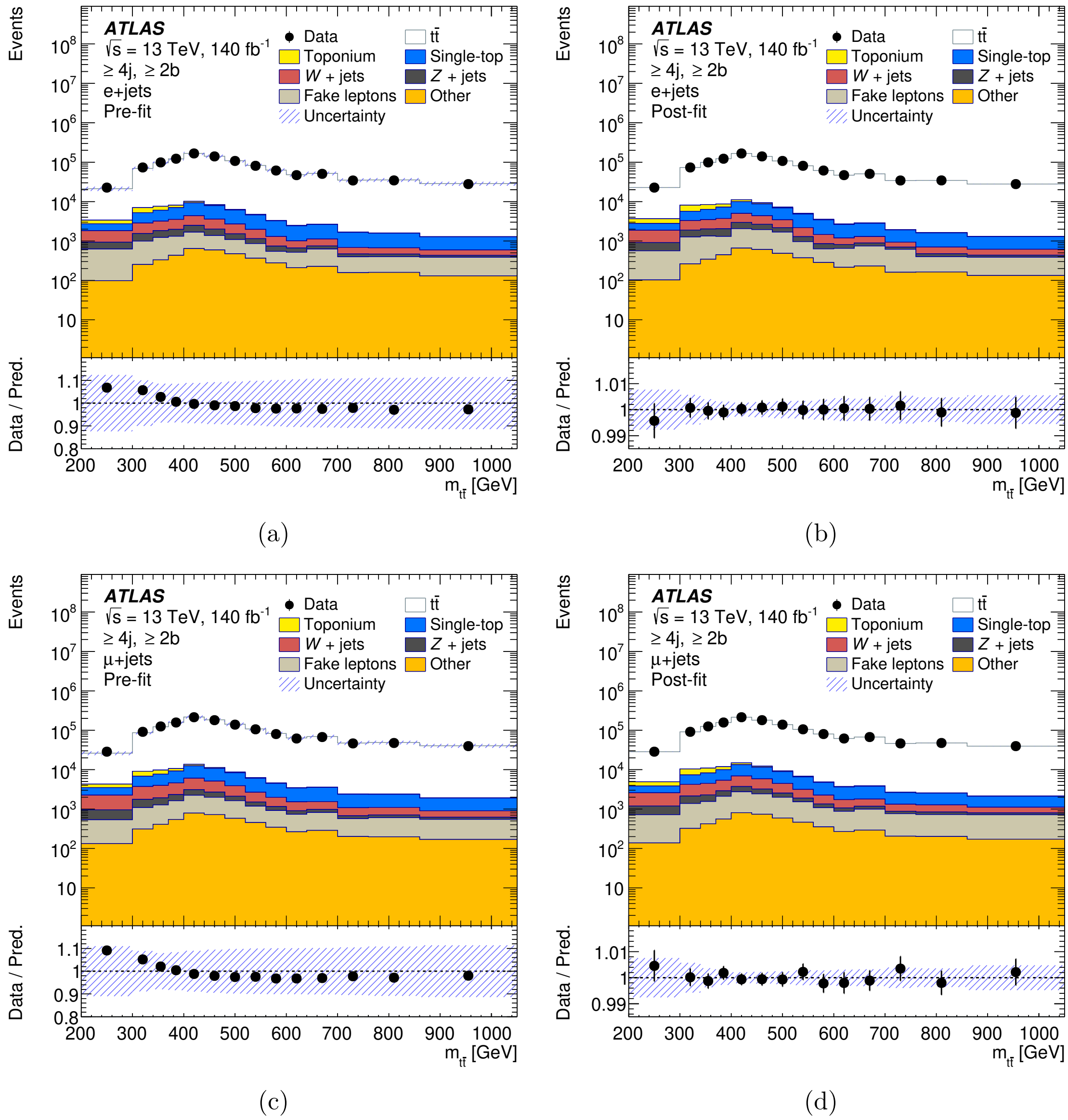

Figure 5. The $m_{t\bar{t}}$ distributions (a), (c) before the fit and (b), (d) after the combined fit, for e+jets and μ+jets SRs, respectively. The $t\bar{t}$ signal in the plots corresponds to $Y_t = 1$. The shaded bands represent the contribution of statistical and systematic uncertainties. The bottom panel in the figures show the ratio of the data over the total prediction.

figure 6. The Y_t^2 values at $-\Delta \ln L = 0.5$ obtained from the likelihood scans give the associated $\pm 1\sigma$ uncertainties.

A summary of the Y_t^2 obtained from a fit to e+jets SR only, μ+jets SR only and the simultaneous fit to both SRs (combined fit) is shown in table 1. The observed value of Y_t^2 is 1.3 ± 1.7, which is consistent with the Standard Model expectation of $Y_t^2 = 1$. A 95% confidence level (CL) upper limit on Y_t^2 using a modified frequentist $\mathrm{CL_s}$ procedure [110] is also obtained, considering only the physical region of $Y_t^2 > 0$. Subsequently, the upper limits on Y_t for the individual SR fits as well as the combined fit are obtained, which are

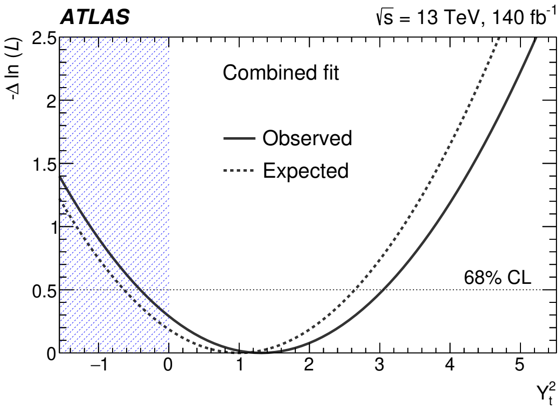

Figure 6. The observed and expected negative log-likelihood Y_t^2 scans for the combined fit. The scan minimum shows the best-fit Y_t^2. The horizontal line corresponds to the $\pm 1\sigma$ uncertainty in Y_t^2. The shaded region corresponds to the negative Y_t^2 values, which are unphysical and are only used to improve the fit stability.

Region	**Expected** Y_t^2	**Observed** Y_t^2	**95%** $\mathrm{CL_s}$ **upper limit on** Y_t	
			Expected	**Observed**
e+jets	$1.0^{+2.1}_{-2.0}$	$1.3^{+2.2}_{-2.1}$	< 2.3	< 2.4
μ+jets	$1.0^{+1.8}_{-1.8}$	$1.1^{+1.9}_{-1.9}$	< 2.1	< 2.2
Combined	$1.0^{+1.6}_{-1.6}$	$1.3^{+1.7}_{-1.7}$	< 2.1	< 2.1

Table 1. Summary of the results for the individual SR and the combined fit. The expected and observed best fit values for Y_t^2 with uncertainty and their corresponding 95% CL upper limits on Y_t are shown.

also summarised in table 1. This results in observed (expected) limits of $Y_t < 2.4$ (2.3) for electrons, $Y_t < 2.2$ (2.1) for muons, and $Y_t < 2.1$ (2.1) for the combined result, at 95% CL.

Figure 7 shows the shifts relative to pre-fit values, the constraints and the impact on Y_t^2 of the nuisance parameters (NPs) with the largest contribution to the total uncertainty in the combined fit. The impacts of individual NPs on the measurement are extracted from the covariance matrix [111]. The measurement is dominated by systematic uncertainties, where the largest impact comes from the $t\bar{t}$ modelling, specifically from the μ_{f} scale variation, followed by the JES modelling. The top quark mass and the h_{damp} variation show an impact of a similar order. The strongest constraints are observed from the NPs associated with $t\bar{t}$ modelling. The NNLO reweighting uncertainty is the most constrained, followed by the parton shower and hadronisation uncertainty for ≥ 5 jets. Table 2 summarises the impact from different categories of uncertainty sources. The NPs associated with $t\bar{t}$ modelling, JES, and background modelling constitute the dominant contributions to the total systematic uncertainty. Among the background modelling uncertainties, the largest contribution arises from the uncertainty in the fake-lepton background estimate. The impact of the toponium normalisation uncertainty is negligible, at the level of ± 0.1 on Y_t^2.

JHEP01(2026)117

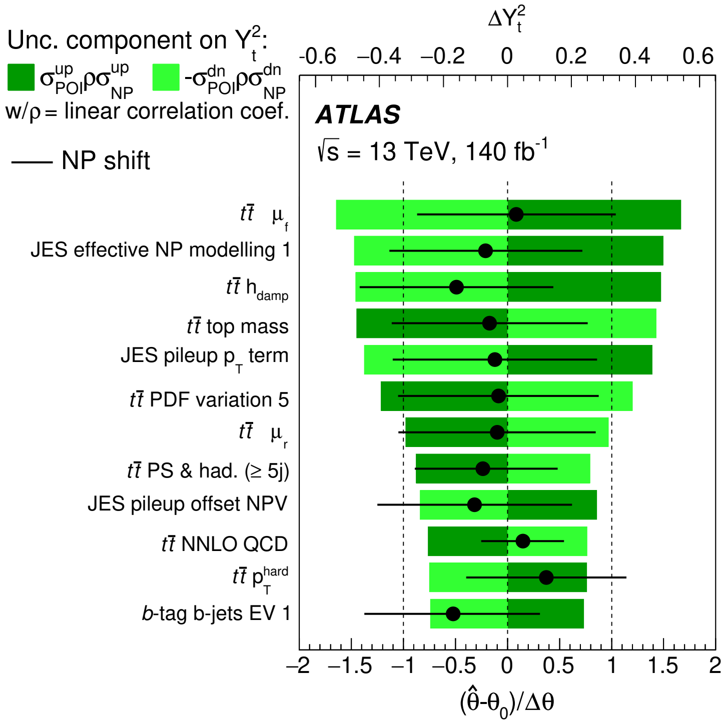

Figure 7. Ranking of the most impactful NPs in the combined fit with Y_t^2 as the parameter of interest. The rectangular bars show the impact of each NP, given by the ΔY_t^2 corresponding to the top scale, estimated from the off-diagonal elements of the fit covariance matrix [111]. The points show the ratio of the difference between the fitted value of the NPs $\hat{\theta}$, relative to their nominal value θ_0, over the pre-fit uncertainty $\Delta\theta$. The solid lines show the NP post-fit uncertainties corresponding to the bottom scale.

Uncertainty category	**Impact on Y_t^2**
$t\bar{t}$ modelling	± 1.2
Jet energy scale	± 0.8
Background modelling	± 0.6
Jet energy resolution	± 0.4
b-tagging scale factor	± 0.3
Others	± 0.3
Statistical uncertainty	± 0.4
Total systematic uncertainty	± 1.7

Table 2. Impact of the different categories of systematic uncertainties. The impacts of the NPs on Y_t^2 in a given category are summed in quadrature. The category "Others" includes uncertainties in luminosity, pileup modelling, jet vertex tagger efficiency, E_T^{miss}, leptons and the MC statistical uncertainty. The statistical uncertainty in Y_t^2 is obtained by subtracting the total systematic uncertainty from the total uncertainty in quadrature.

As discussed in section 5.2, this paper adopts a multiplicative approach to incorporate electroweak corrections, while the additive approach is considered as a systematic uncertainty. This uncertainty depends upon the value of Y_t, and has been evaluated for $Y_t = 1$ in the fit. A test performed assuming this uncertainty at $Y_t = 2$ results in a 6% increase in the upper limit on Y_t.

This result represents the first ATLAS measurement of Y_t from the $t\bar{t}$ production threshold region, consistent with the prediction of the Standard Model and with corresponding measurements by CMS [17, 18]. It is also consistent with all other direct and indirect measurements of Y_t.

8 Conclusion

The top-quark Yukawa coupling strength Y_t is extracted from the differential $t\bar{t}$ cross-section in events with a single lepton in the final state. This paper presents the first ATLAS measurement of Y_t in the $t\bar{t}$ production threshold region. The analysis uses a $\sqrt{s} = 13$ TeV pp collision dataset collected at the LHC and corresponding to an integrated luminosity of 140 fb^{-1}. The parameter of interest, Y_t^2, is extracted from a template-based profile likelihood fit to the invariant mass of the $t\bar{t}$ pair, where the $t\bar{t}$ production threshold is particularly sensitive to virtual electroweak corrections, including the Higgs boson exchange between two top quarks. The electroweak corrections, including the free Y_t parameter, are applied using HATHOR on top of NLO QCD predictions using POWHEG BOX-v2. The fitted $Y_t^2 = 1.3 \pm 1.7$ is in good agreement with the Standard Model prediction of $Y_t^2 = 1$ as well as with the CMS measurements in the single-lepton [17] and dilepton channels [18]. Normalising over the physical region, $Y_t^2 > 0$, yields a 95% CL limit of $Y_t < 2.1$. The presented measurement provides a complementary approach compared to other indirect measurements with a similar sensitivity to constrain the Y_t coupling strength.

Acknowledgments

We thank CERN for the very successful operation of the LHC and its injectors, as well as the support staff at CERN and at our institutions worldwide without whom ATLAS could not be operated efficiently.

The crucial computing support from all WLCG partners is acknowledged gratefully, in particular from CERN, the ATLAS Tier-1 facilities at TRIUMF/SFU (Canada), NDGF (Denmark, Norway, Sweden), CC-IN2P3 (France), KIT/GridKA (Germany), INFN-CNAF (Italy), NL-T1 (Netherlands), PIC (Spain), RAL (U.K.) and BNL (U.S.A.), the Tier-2 facilities worldwide and large non-WLCG resource providers. Major contributors of computing resources are listed in ref. [112].

We gratefully acknowledge the support of ANPCyT, Argentina; YerPhI, Armenia; ARC, Australia; BMWFW and FWF, Austria; ANAS, Azerbaijan; CNPq and FAPESP, Brazil; NSERC, NRC and CFI, Canada; CERN; ANID, Chile; CAS, MOST and NSFC, China; Minciencias, Colombia; MEYS CR, Czech Republic; DNRF and DNSRC, Denmark; IN2P3-CNRS and CEA-DRF/IRFU, France; SRNSFG, Georgia; BMFTR, HGF and MPG, Germany; GSRI, Greece; RGC and Hong Kong SAR, China; ICHEP and Academy of Sciences and

JHEP01(2026)117

Humanities, Israel; INFN, Italy; MEXT and JSPS, Japan; CNRST, Morocco; NWO, Netherlands; RCN, Norway; MNiSW, Poland; FCT, Portugal; MNE/IFA, Romania; MSTDI, Serbia; MSSR, Slovakia; ARIS and MVZI, Slovenia; DSI/NRF, South Africa; MICIU/AEI, Spain; SRC and Wallenberg Foundation, Sweden; SERI, SNSF and Cantons of Bern and Geneva, Switzerland; NSTC, Taipei; TENMAK, Türkiye; STFC/UKRI, United Kingdom; DOE and NSF, United States of America.

Individual groups and members have received support from BCKDF, CANARIE, CRC and DRAC, Canada; CERN-CZ, FORTE and PRIMUS, Czech Republic; COST, ERC, ERDF, Horizon 2020, ICSC-NextGenerationEU and Marie Skłodowska-Curie Actions, European Union; Investissements d'Avenir Labex, Investissements d'Avenir Idex and ANR, France; DFG and AvH Foundation, Germany; Herakleitos, Thales and Aristeia programmes co-financed by EU-ESF and the Greek NSRF, Greece; BSF-NSF and MINERVA, Israel; NCN and NAWA, Poland; La Caixa Banking Foundation, CERCA Programme Generalitat de Catalunya and PROMETEO and GenT Programmes Generalitat Valenciana, Spain; Göran Gustafssons Stiftelse, Sweden; The Royal Society and Leverhulme Trust, United Kingdom.

In addition, individual members wish to acknowledge support from CERN: European Organization for Nuclear Research (CERN DOCT); Chile: Agencia Nacional de Investigación y Desarrollo (FONDECYT 1230812, FONDECYT 1240864, Fondecyt 3240661, Fondecyt Regular 1240721); China: Chinese Ministry of Science and Technology (MOST-2023YFA1605700, MOST-2023YFA1609300), National Natural Science Foundation of China (NSFC – 12175119, NSFC 12275265); Czech Republic: Czech Science Foundation (GACR – 24-11373S), Ministry of Education Youth and Sports (ERC-CZ-LL2327, FORTE CZ.02.01.01/00/22_008/0004632), PRIMUS Research Programme (PRIMUS/21/SCI/017); EU: H2020 European Research Council (ERC – 101002463); European Union: European Research Council (BARD No. 101116429, ERC – 948254, ERC 101089007), European Regional Development Fund (SMASH COFUND 101081355, SLO ERDF), European Union, Future Artificial Intelligence Research (FAIR-NextGenerationEU PE00000013), Italian Center for High Performance Computing, Big Data and Quantum Computing (ICSC, NextGenerationEU); France: Agence Nationale de la Recherche (ANR-21-CE31-0022, ANR-22-EDIR-0002, ANR-24-CE31-0504-01); Germany: Deutsche Forschungsgemeinschaft (DFG – 469666862, DFG – CR 312/5-2); China: Research Grants Council (GRF); Italy: Istituto Nazionale di Fisica Nucleare (ICSC, NextGenerationEU), Ministero dell'Università e della Ricerca (NextGenEU 153D23001490006 M4C2.1.1, NextGenEU I53D23000820006 M4C2.1.1, NextGenEU I53D23001490006 M4C2.1.1, SOE2024_0000023); Japan: Japan Society for the Promotion of Science (JSPS KAKENHI JP22H01227, JSPS KAKENHI JP22H04944, JSPS KAKENHI JP22KK0227, JSPS KAKENHI JP24K23939, JSPS KAKENHI JP24KK0251, JSPS KAKENHI JP25H00650, JSPS KAKENHI JP25H01291, JSPS KAKENHI JP25K01023); Norway: Research Council of Norway (RCN-314472); Poland: Ministry of Science and Higher Education (IDUB AGH, POB8, D4 no 9722), Polish National Science Centre (NCN 2021/42/E/ST2/00350, NCN OPUS 2023/51/B/ST2/02507, NCN UMO-2019/34/E/ST2/00393, UMO-2022/47/O/ST2/00148, UMO-2023/49/B/ST2/04085, UMO-2023/51/B/ST2/00920, UMO-2024/53/N/ST2/00869); Portugal: Foundation for Science and Technology (FCT); Spain: Ministry of Science and Innovation (MCIN & NextGenEU PCI2022-135018-2, MICIN & FEDER PID2021-125273NB,

RYC2019-028510-I, RYC2020-030254-I, RYC2021-031273-I, RYC2022-038164-I); Sweden: Carl Trygger Foundation (Carl Trygger Foundation CTS 22:2312), Swedish Research Council (Swedish Research Council 2023-04654, VR 2021-03651, VR 2022-03845, VR 2022-04683, VR 2023-03403, VR 2024-05451), Knut and Alice Wallenberg Foundation (KAW 2018.0458, KAW 2022.0358, KAW 2023.0366); Switzerland: Swiss National Science Foundation (SNSF – PCEFP2_194658); United Kingdom: Royal Society (NIF-R1-231091); United States of America: U.S. Department of Energy (ECA DE-AC02-76SF00515), Neubauer Family Foundation.

Data Availability Statement. The public release of data supporting the findings of this article will follow the CERN Open Data Policy [113]. Inquiries about plots and tables associated with this article can be addressed to atlas.publications@cern.ch.

Code Availability Statement. This article has associated code in a code repository. The ATLAS Collaboration's Athena software, including the configuration of the event generators, is open source (`http://gitlab.cern.ch/atlas/athena`).

References

[1] F. Englert and R. Brout, *Broken Symmetry and the Mass of Gauge Vector Mesons*, *Phys. Rev. Lett.* **13** (1964) 321 [INSPIRE].

[2] P.W. Higgs, *Broken symmetries, massless particles and gauge fields*, *Phys. Lett.* **12** (1964) 132 [INSPIRE].

[3] P.W. Higgs, *Broken Symmetries and the Masses of Gauge Bosons*, *Phys. Rev. Lett.* **13** (1964) 508 [INSPIRE].

[4] G.S. Guralnik, C.R. Hagen and T.W.B. Kibble, *Global Conservation Laws and Massless Particles*, *Phys. Rev. Lett.* **13** (1964) 585 [INSPIRE].

[5] P.W. Higgs, *Spontaneous Symmetry Breakdown without Massless Bosons*, *Phys. Rev.* **145** (1966) 1156 [INSPIRE].

[6] T.W.B. Kibble, *Symmetry Breaking in Non-Abelian Gauge Theories*, *Phys. Rev.* **155** (1967) 1554 [INSPIRE].

[7] Particle Data Group collaboration, *Review of particle physics*, *Phys. Rev. D* **110** (2024) 030001 [INSPIRE].

[8] ATLAS collaboration, *Measurement of the associated production of a top-antitop-quark pair and a Higgs boson decaying into a $b\bar{b}$ pair in pp collisions at $\sqrt{s} = 13$ TeV using the ATLAS detector at the LHC*, *Eur. Phys. J. C* **85** (2025) 210 [arXiv:2407.10904] [INSPIRE].

[9] ATLAS collaboration, *A detailed map of Higgs boson interactions by the ATLAS experiment ten years after the discovery*, *Nature* **607** (2022) 52 [*Erratum ibid.* **612** (2022) E24] [arXiv:2207.00092] [INSPIRE].

[10] CMS collaboration, *A portrait of the Higgs boson by the CMS experiment ten years after the discovery*, *Nature* **607** (2022) 60 [arXiv:2207.00043] [INSPIRE].

JHEP01(2026)117

[11] ATLAS collaboration, *Observation of four-top-quark production in the multilepton final state with the ATLAS detector*, *Eur. Phys. J. C* **83** (2023) 496 [*Erratum ibid.* **84** (2024) 156] [arXiv:2303.15061] [INSPIRE].

[12] CMS collaboration, *Search for production of four top quarks in final states with same-sign or multiple leptons in proton-proton collisions at $\sqrt{s} = 13$ TeV*, *Eur. Phys. J. C* **80** (2020) 75 [arXiv:1908.06463] [INSPIRE].

[13] J.H. Kühn, A. Scharf and P. Uwer, *Weak Interactions in Top-Quark Pair Production at Hadron Colliders: An Update*, *Phys. Rev. D* **91** (2015) 014020 [arXiv:1305.5773] [INSPIRE].

[14] F. Maltoni, D. Pagani and S. Tentori, *Top-quark pair production as a probe of light top-philic scalars and anomalous Higgs interactions*, *JHEP* **09** (2024) 098 [arXiv:2406.06694] [INSPIRE].

[15] ATLAS collaboration, *Search for $t\bar{t}H/A \to t\bar{t}t\bar{t}$ production in proton-proton collisions at $\sqrt{s} = 13$ TeV with the ATLAS detector*, *Eur. Phys. J. C* **85** (2025) 573 [arXiv:2408.17164] [INSPIRE].

[16] ATLAS collaboration, *Search for heavy neutral Higgs bosons decaying into a top quark pair in 140 fb^{-1} of proton-proton collision data at $\sqrt{s} = 13$ TeV with the ATLAS detector*, *JHEP* **08** (2024) 013 [arXiv:2404.18986] [INSPIRE].

[17] CMS collaboration, *Measurement of the top quark Yukawa coupling from $t\bar{t}$ kinematic distributions in the lepton+jets final state in proton-proton collisions at $\sqrt{s} = 13$ TeV*, *Phys. Rev. D* **100** (2019) 072007 [arXiv:1907.01590] [INSPIRE].

[18] CMS collaboration, *Measurement of the top quark Yukawa coupling from $t\bar{t}$ kinematic distributions in the dilepton final state in proton-proton collisions at $\sqrt{s} = 13$ TeV*, *Phys. Rev. D* **102** (2020) 092013 [arXiv:2009.07123] [INSPIRE].

[19] J.H. Kühn, A. Scharf and P. Uwer, *Electroweak effects in top-quark pair production at hadron colliders*, *Eur. Phys. J. C* **51** (2007) 37 [hep-ph/0610335] [INSPIRE].

[20] J.H. Kühn, A. Scharf and P. Uwer, *Electroweak corrections to top-quark pair production in quark-antiquark annihilation*, *Eur. Phys. J. C* **45** (2006) 139 [hep-ph/0508092] [INSPIRE].

[21] M. Aliev et al., *Hathor version 2.1-b3*, https://www.physik.hu-berlin.de/de/pep/tools/hathor.html.

[22] ATLAS collaboration, *The ATLAS Experiment at the CERN Large Hadron Collider*, 2008 *JINST* **3** S08003 [INSPIRE].

[23] L. Evans and P. Bryant, *LHC Machine*, 2008 *JINST* **3** S08001 [INSPIRE].

[24] ATLAS collaboration, *ATLAS Insertable B-Layer: Technical Design Report*, ATLAS-TDR-19 (2010).

[25] ATLAS IBL collaboration, *Production and Integration of the ATLAS Insertable B-Layer*, 2018 *JINST* **13** T05008 [arXiv:1803.00844] [INSPIRE].

[26] G. Avoni et al., *The new LUCID-2 detector for luminosity measurement and monitoring in ATLAS*, 2018 *JINST* **13** P07017 [INSPIRE].

[27] ATLAS collaboration, *Performance of the ATLAS Trigger System in 2015*, *Eur. Phys. J. C* **77** (2017) 317 [arXiv:1611.09661] [INSPIRE].

[28] ATLAS collaboration, *Software and computing for Run 3 of the ATLAS experiment at the LHC*, *Eur. Phys. J. C* **85** (2025) 234 [arXiv:2404.06335] [INSPIRE].

[29] ATLAS collaboration, *ATLAS data quality operations and performance for 2015–2018 data-taking*, 2020 *JINST* **15** P04003 [arXiv:1911.04632] [INSPIRE].

JHEP01(2026)117

[30] ATLAS collaboration, *The ATLAS Simulation Infrastructure*, Eur. Phys. J. C **70** (2010) 823 [arXiv:1005.4568] [INSPIRE].

[31] GEANT4 collaboration, *Geant4 — a simulation toolkit*, Nucl. Instrum. Meth. A **506** (2003) 250 [INSPIRE].

[32] ATLAS collaboration, *The simulation principle and performance of the ATLAS fast calorimeter simulation FastCaloSim*, ATL-PHYS-PUB-2010-013 (2010) [INSPIRE].

[33] T. Sjöstrand, S. Mrenna and P.Z. Skands, *A Brief Introduction to PYTHIA 8.1*, Comput. Phys. Commun. **178** (2008) 852 [arXiv:0710.3820] [INSPIRE].

[34] R.D. Ball et al., *Parton distributions with LHC data*, Nucl. Phys. B **867** (2013) 244 [arXiv:1207.1303] [INSPIRE].

[35] ATLAS collaboration, *The Pythia 8 A3 tune description of ATLAS minimum bias and inelastic measurements incorporating the Donnachie-Landshoff diffractive model*, ATL-PHYS-PUB-2016-017 (2016) [INSPIRE].

[36] D.J. Lange, *The EvtGen particle decay simulation package*, Nucl. Instrum. Meth. A **462** (2001) 152 [INSPIRE].

[37] T. Gleisberg et al., *Event generation with SHERPA 1.1*, JHEP **02** (2009) 007 [arXiv:0811.4622] [INSPIRE].

[38] P. Nason, *A new method for combining NLO QCD with shower Monte Carlo algorithms*, JHEP **11** (2004) 040 [hep-ph/0409146] [INSPIRE].

[39] S. Frixione, P. Nason and C. Oleari, *Matching NLO QCD computations with Parton Shower simulations: the POWHEG method*, JHEP **11** (2007) 070 [arXiv:0709.2092] [INSPIRE].

[40] S. Alioli, P. Nason, C. Oleari and E. Re, *A general framework for implementing NLO calculations in shower Monte Carlo programs: the POWHEG BOX*, JHEP **06** (2010) 043 [arXiv:1002.2581] [INSPIRE].

[41] NNPDF collaboration, *Parton distributions for the LHC Run II*, JHEP **04** (2015) 040 [arXiv:1410.8849] [INSPIRE].

[42] T. Sjöstrand et al., *An introduction to PYTHIA 8.2*, Comput. Phys. Commun. **191** (2015) 159 [arXiv:1410.3012] [INSPIRE].

[43] ATLAS collaboration, *ATLAS Pythia 8 tunes to 7 TeV data*, ATL-PHYS-PUB-2014-021 (2014) [INSPIRE].

[44] ATLAS collaboration, *Studies on the improvement of the matching uncertainty definition in top-quark processes simulated with Powheg+Pythia8*, ATL-PHYS-PUB-2023-029 (2023) [INSPIRE].

[45] J. Bellm et al., *Herwig 7.0/Herwig++ 3.0 release note*, Eur. Phys. J. C **76** (2016) 196 [arXiv:1512.01178] [INSPIRE].

[46] M. Bähr et al., *Herwig++ Physics and Manual*, Eur. Phys. J. C **58** (2008) 639 [arXiv:0803.0883] [INSPIRE].

[47] L.A. Harland-Lang, A.D. Martin, P. Motylinski and R.S. Thorne, *Parton distributions in the LHC era: MMHT 2014 PDFs*, Eur. Phys. J. C **75** (2015) 204 [arXiv:1412.3989] [INSPIRE].

[48] S. Frixione, E. Laenen, P. Motylinski and B.R. Webber, *Angular correlations of lepton pairs from vector boson and top quark decays in Monte Carlo simulations*, JHEP **04** (2007) 081 [hep-ph/0702198] [INSPIRE].

[49] P. Artoisenet, R. Frederix, O. Mattelaer and R. Rietkerk, *Automatic spin-entangled decays of heavy resonances in Monte Carlo simulations*, JHEP **03** (2013) 015 [arXiv:1212.3460] [INSPIRE].

[50] M. Czakon and A. Mitov, *Top++: A Program for the Calculation of the Top-Pair Cross-Section at Hadron Colliders*, Comput. Phys. Commun. **185** (2014) 2930 [arXiv:1112.5675] [INSPIRE].

[51] M. Beneke, P. Falgari, S. Klein and C. Schwinn, *Hadronic top-quark pair production with NNLL threshold resummation*, Nucl. Phys. B **855** (2012) 695 [arXiv:1109.1536] [INSPIRE].

[52] M. Cacciari et al., *Top-pair production at hadron colliders with next-to-next-to-leading logarithmic soft-gluon resummation*, Phys. Lett. B **710** (2012) 612 [arXiv:1111.5869] [INSPIRE].

[53] P. Bärnreuther, M. Czakon and A. Mitov, *Percent Level Precision Physics at the Tevatron: First Genuine NNLO QCD Corrections to $q\bar{q} \to t\bar{t} + X$*, Phys. Rev. Lett. **109** (2012) 132001 [arXiv:1204.5201] [INSPIRE].

[54] M. Czakon and A. Mitov, *NNLO corrections to top-pair production at hadron colliders: the all-fermionic scattering channels*, JHEP **12** (2012) 054 [arXiv:1207.0236] [INSPIRE].

[55] M. Czakon and A. Mitov, *NNLO corrections to top pair production at hadron colliders: the quark-gluon reaction*, JHEP **01** (2013) 080 [arXiv:1210.6832] [INSPIRE].

[56] M. Czakon, P. Fiedler and A. Mitov, *Total Top-Quark Pair-Production Cross Section at Hadron Colliders Through $\mathcal{O}(\alpha_S^4)$*, Phys. Rev. Lett. **110** (2013) 252004 [arXiv:1303.6254] [INSPIRE].

[57] S. Catani et al., *Top-quark pair hadroproduction at next-to-next-to-leading order in QCD*, Phys. Rev. D **99** (2019) 051501 [arXiv:1901.04005] [INSPIRE].

[58] S. Catani et al., *Top-quark pair production at the LHC: Fully differential QCD predictions at NNLO*, JHEP **07** (2019) 100 [arXiv:1906.06535] [INSPIRE].

[59] M. Grazzini, S. Kallweit and M. Wiesemann, *Fully differential NNLO computations with MATRIX*, Eur. Phys. J. C **78** (2018) 537 [arXiv:1711.06631] [INSPIRE].

[60] A. Denner, S. Dittmaier and L. Hofer, *Collier: A fortran-based complex one-loop library in extended regularizations*, Comput. Phys. Commun. **212** (2017) 220 [arXiv:1604.06792] [INSPIRE].

[61] F. Cascioli, P. Maierhöfer and S. Pozzorini, *Scattering Amplitudes with Open Loops*, Phys. Rev. Lett. **108** (2012) 111601 [arXiv:1111.5206] [INSPIRE].

[62] F. Buccioni et al., *OpenLoops 2*, Eur. Phys. J. C **79** (2019) 866 [arXiv:1907.13071] [INSPIRE].

[63] F. Buccioni, S. Pozzorini and M. Zoller, *On-the-fly reduction of open loops*, Eur. Phys. J. C **78** (2018) 70 [arXiv:1710.11452] [INSPIRE].

[64] P. Bärnreuther, M. Czakon and P. Fiedler, *Virtual amplitudes and threshold behaviour of hadronic top-quark pair-production cross sections*, JHEP **02** (2014) 078 [arXiv:1312.6279] [INSPIRE].

[65] J. Mazzitelli et al., *Top-pair production at the LHC with MINNLO$_{PS}$*, JHEP **04** (2022) 079 [arXiv:2112.12135] [INSPIRE].

[66] CMS collaboration, *Observation of a pseudoscalar excess at the top quark pair production threshold*, Rept. Prog. Phys. **88** (2025) 087801 [arXiv:2503.22382] [INSPIRE].

[67] B. Fuks, K. Hagiwara, K. Ma and Y.-J. Zheng, *Signatures of toponium formation in LHC run 2 data*, Phys. Rev. D **104** (2021) 034023 [arXiv:2102.11281] [INSPIRE].

[68] F. Maltoni, C. Severi, S. Tentori and E. Vryonidou, *Quantum detection of new physics in top-quark pair production at the LHC*, JHEP **03** (2024) 099 [arXiv:2401.08751] [INSPIRE].

[69] K. Hagiwara, Y. Sumino and H. Yokoya, *Bound-state Effects on Top Quark Production at Hadron Colliders*, Phys. Lett. B **666** (2008) 71 [arXiv:0804.1014] [INSPIRE].

[70] Y. Sumino and H. Yokoya, *Bound-state effects on kinematical distributions of top quarks at hadron colliders*, JHEP **09** (2010) 034 [*Erratum ibid.* **06** (2016) 037] [arXiv:1007.0075] [INSPIRE].

[71] C. Bierlich et al., *A comprehensive guide to the physics and usage of PYTHIA 8.3*, SciPost Phys. Codeb. **2022** (2022) 8 [arXiv:2203.11601] [INSPIRE].

[72] S. Frixione et al., *Single-top hadroproduction in association with a W boson*, JHEP **07** (2008) 029 [arXiv:0805.3067] [INSPIRE].

[73] ATLAS collaboration, *Studies on top-quark Monte Carlo modelling for Top2016*, ATL-PHYS-PUB-2016-020 (2016) [INSPIRE].

[74] J. Campbell, T. Neumann and Z. Sullivan, *Single-top-quark production in the t-channel at NNLO*, JHEP **02** (2021) 040 [arXiv:2012.01574] [INSPIRE].

[75] N. Kidonakis, *NNLL resummation for s-channel single top quark production*, Phys. Rev. D **81** (2010) 054028 [arXiv:1001.5034] [INSPIRE].

[76] N. Kidonakis and N. Yamanaka, *Higher-order corrections for tW production at high-energy hadron colliders*, JHEP **05** (2021) 278 [arXiv:2102.11300] [INSPIRE].

[77] SHERPA collaboration, *Event Generation with Sherpa 2.2*, SciPost Phys. **7** (2019) 034 [arXiv:1905.09127] [INSPIRE].

[78] T. Gleisberg and S. Hoeche, *Comix, a new matrix element generator*, JHEP **12** (2008) 039 [arXiv:0808.3674] [INSPIRE].

[79] S. Hoeche, F. Krauss, M. Schönherr and F. Siegert, *QCD matrix elements + parton showers: The NLO case*, JHEP **04** (2013) 027 [arXiv:1207.5030] [INSPIRE].

[80] ATLAS collaboration, *Inclusive $W^{\pm}$ and Z^0 cross sections at next-to-next-to leading order QCD for the ATLAS experiment*, ATL-PHYS-PUB-2023-026 (2023) [INSPIRE].

[81] C. Anastasiou, L.J. Dixon, K. Melnikov and F. Petriello, *High precision QCD at hadron colliders: Electroweak gauge boson rapidity distributions at NNLO*, Phys. Rev. D **69** (2004) 094008 [hep-ph/0312266] [INSPIRE].

[82] J.M. Campbell and R.K. Ellis, *An update on vector boson pair production at hadron colliders*, Phys. Rev. D **60** (1999) 113006 [hep-ph/9905386] [INSPIRE].

[83] J. Alwall et al., *The automated computation of tree-level and next-to-leading order differential cross sections, and their matching to parton shower simulations*, JHEP **07** (2014) 079 [arXiv:1405.0301] [INSPIRE].

[84] H.B. Hartanto, B. Jäger, L. Reina and D. Wackeroth, *Higgs boson production in association with top quarks in the POWHEG BOX*, Phys. Rev. D **91** (2015) 094003 [arXiv:1501.04498] [INSPIRE].

[85] LHC HIGGS CROSS SECTION WORKING GROUP collaboration, *Handbook of LHC Higgs Cross Sections: 4. Deciphering the Nature of the Higgs Sector*, CERN Yellow Rep. Monogr. **2** (2017) 1 [arXiv:1610.07922] [INSPIRE].

[86] ATLAS collaboration, *Vertex Reconstruction Performance of the ATLAS Detector at $\sqrt{s} = 13$ TeV*, ATL-PHYS-PUB-2015-026 (2015) [INSPIRE].

[87] ATLAS collaboration, *Electron and photon performance measurements with the ATLAS detector using the 2015–2017 LHC proton-proton collision data*, 2019 *JINST* **14** P12006 [arXiv:1908.00005] [INSPIRE].

[88] ATLAS collaboration, *Muon reconstruction and identification efficiency in ATLAS using the full Run 2 pp collision data set at* $\sqrt{s} = 13$ *TeV*, *Eur. Phys. J. C* **81** (2021) 578 [arXiv:2012.00578] [INSPIRE].

[89] ATLAS collaboration, *Muon reconstruction performance of the ATLAS detector in proton-proton collision data at* $\sqrt{s} = 13$ *TeV*, *Eur. Phys. J. C* **76** (2016) 292 [arXiv:1603.05598] [INSPIRE].

[90] ATLAS collaboration, *Jet reconstruction and performance using particle flow with the ATLAS Detector*, *Eur. Phys. J. C* **77** (2017) 466 [arXiv:1703.10485] [INSPIRE].

[91] ATLAS collaboration, *Jet energy scale and resolution measured in proton-proton collisions at* $\sqrt{s} = 13$ *TeV with the ATLAS detector*, *Eur. Phys. J. C* **81** (2021) 689 [arXiv:2007.02645] [INSPIRE].

[92] M. Cacciari, G.P. Salam and G. Soyez, *The anti-*k_t *jet clustering algorithm*, *JHEP* **04** (2008) 063 [arXiv:0802.1189] [INSPIRE].

[93] M. Cacciari, G.P. Salam and G. Soyez, *FastJet User Manual*, *Eur. Phys. J. C* **72** (2012) 1896 [arXiv:1111.6097] [INSPIRE].

[94] ATLAS collaboration, *Performance of pile-up mitigation techniques for jets in pp collisions at* $\sqrt{s} = 8$ *TeV using the ATLAS detector*, *Eur. Phys. J. C* **76** (2016) 581 [arXiv:1510.03823] [INSPIRE].

[95] ATLAS collaboration, *ATLAS flavour-tagging algorithms for the LHC Run 2 pp collision dataset*, *Eur. Phys. J. C* **83** (2023) 681 [arXiv:2211.16345] [INSPIRE].

[96] ATLAS collaboration, *The performance of missing transverse momentum reconstruction and its significance with the ATLAS detector using 140 fb*$^{-1}$ *of* $\sqrt{s} = 13$ *TeV pp collisions*, *Eur. Phys. J. C* **85** (2025) 606 [arXiv:2402.05858] [INSPIRE].

[97] ATLAS collaboration, *Performance of electron and photon triggers in ATLAS during LHC Run 2*, *Eur. Phys. J. C* **80** (2020) 47 [arXiv:1909.00761] [INSPIRE].

[98] ATLAS collaboration, *Performance of the ATLAS muon triggers in Run 2*, 2020 *JINST* **15** P09015 [arXiv:2004.13447] [INSPIRE].

[99] ATLAS collaboration, *Tools for estimating fake/non-prompt lepton backgrounds with the ATLAS detector at the LHC*, 2023 *JINST* **18** T11004 [arXiv:2211.16178] [INSPIRE].

[100] ATLAS collaboration, *Luminosity determination in pp collisions at* $\sqrt{s} = 13$ *TeV using the ATLAS detector at the LHC*, *Eur. Phys. J. C* **83** (2023) 982 [arXiv:2212.09379] [INSPIRE].

[101] ATLAS collaboration, *Studies of the muon momentum calibration and performance of the ATLAS detector with pp collisions at* $\sqrt{s} = 13$ *TeV*, *Eur. Phys. J. C* **83** (2023) 686 [arXiv:2212.07338] [INSPIRE].

[102] ATLAS collaboration, *Dependence of the Jet Energy Scale on the Particle Content of Hadronic Jets in the ATLAS Detector Simulation*, ATL-PHYS-PUB-2022-021 (2022) [INSPIRE].

[103] ATLAS collaboration, *ATLAS b-jet identification performance and efficiency measurement with* $t\bar{t}$ *events in pp collisions at* $\sqrt{s} = 13$ *TeV*, *Eur. Phys. J. C* **79** (2019) 970 [arXiv:1907.05120] [INSPIRE].

[104] ATLAS collaboration, *Measurement of the c-jet mistagging efficiency in $t\bar{t}$ events using pp collision data at $\sqrt{s} = 13$ TeV collected with the ATLAS detector*, Eur. Phys. J. C **82** (2022) 95 [arXiv:2109.10627] [INSPIRE].

[105] ATLAS collaboration, *Calibration of the light-flavour jet mistagging efficiency of the b-tagging algorithms with Z+jets events using 139 fb^{-1} of ATLAS proton-proton collision data at* $\sqrt{s} = 13$ *TeV*, Eur. Phys. J. C **83** (2023) 728 [arXiv:2301.06319] [INSPIRE].

[106] J. Butterworth et al., *PDF4LHC recommendations for LHC Run II*, J. Phys. G **43** (2016) 023001 [arXiv:1510.03865] [INSPIRE].

[107] ATLAS collaboration, *ATLAS simulation of boson plus jets processes in Run 2*, ATL-PHYS-PUB-2017-006 (2017) [INSPIRE].

[108] ROOT collaboration, *HistFactory: A tool for creating statistical models for use with RooFit and RooStats*, CERN-OPEN-2012-016 (2012) [INSPIRE].

[109] M. Aly et al., *TRExFitter*, DOI:10.5281/zenodo.15642614.

[110] A.L. Read, *Presentation of search results: The CL_s technique*, J. Phys. G **28** (2002) 2693 [INSPIRE].

[111] A. Pinto et al., *Uncertainty components in profile likelihood fits*, Eur. Phys. J. C **84** (2024) 593 [arXiv:2307.04007] [INSPIRE].

[112] ATLAS collaboration, *ATLAS Computing Acknowledgements*, ATL-SOFT-PUB-2025-001 (2025) [INSPIRE].

[113] CERN, *CERN Open Data Policy for the LHC Experiments*, CERN-OPEN-2020-013, (2020).

The ATLAS collaboration

G. Aad[103], E. Aakvaag[17], B. Abbott[122], S. Abdelhameed[118a], K. Abeling[55], N.J. Abicht[49], S.H. Abidi[30], M. Aboelela[45], A. Aboulhorma[36e], H. Abramowicz[156], Y. Abulaiti[119], B.S. Acharya[69a,69b,m], A. Ackermann[63a], C. Adam Bourdarios[4], L. Adamczyk[86a], S.V. Addepalli[148], M.J. Addison[102], J. Adelman[117], A. Adiguzel[22c], T. Adye[136], A.A. Affolder[138], Y. Afik[40], M.N. Agaras[13], A. Aggarwal[101], C. Agheorghiesei[28c], F. Ahmadov[39,ad], S. Ahuja[96], S. Ahuja[168], X. Ai[142b], G. Aielli[76a,76b], A. Aikot[168], M. Ait Tamlihat[36e], B. Aitbenchikh[36a], T.P.A. Åkesson[99], A.V. Akimov[150], D. Akiyama[173], N.N. Akolkar[25], S. Aktas[171], G.L. Alberghi[24b], J. Albert[170], U. Alberti[20], P. Albicocco[53], G.L. Albouy[60], S. Alderweireldt[52], Z.L. Alegria[123], M. Aleksa[37], I.N. Aleksandrov[39], C. Alexa[28b], T. Alexopoulos[10], F. Alfonsi[24b], M. Algren[56], M. Alhroob[172], B. Ali[134], H.M.J. Ali[92,w], S. Ali[32], S.W. Alibocus[93], M. Aliev[34c], G. Alimonti[71a], W. Alkakhi[55], C. Allaire[66], B.M.M. Allbrooke[151], D.R. Allen[123], J.S. Allen[102], J.F. Allen[52], P.P. Allport[21], A. Aloisio[72a,72b], F. Alonso[91], C. Alpigiani[141], Z.M.K. Alsolami[92], A. Alvarez Fernandez[101], M. Alves Cardoso[56], M.G. Alviggi[72a,72b], M. Aly[102], Y. Amaral Coutinho[82b], A. Ambler[105], C. Amelung[37], M. Amerl[102], C.G. Ames[110], T. Amezza[129], D. Amidei[107], B. Amini[54], K. Amirie[160], A. Amirkhanov[39], S.P. Amor Dos Santos[132a], K.R. Amos[168], D. Amperiadou[157], S. An[83], C. Anastopoulos[144], T. Andeen[11], J.K. Anders[93], A.C. Anderson[59], A. Andreazza[71a,71b], S. Angelidakis[9], A. Angerami[42], A.V. Anisenkov[39], A. Annovi[74a], C. Antel[37], E. Antipov[150], M. Antonelli[53], F. Anulli[75a], M. Aoki[83], T. Aoki[158], M.A. Aparo[151], L. Aperio Bella[48], M. Apicella[31], C. Appelt[156], A. Apyan[27], M. Arampatzi[10], S.J. Arbiol Val[87], C. Arcangeletti[53], A.T.H. Arce[51], J-F. Arguin[109], S. Argyropoulos[157], J.-H. Arling[48], O. Arnaez[4], H. Arnold[150], G. Artoni[75a,75b], H. Asada[112], K. Asai[120], S. Asatryan[178], N.A. Asbah[37], R.A. Ashby Pickering[172], A.M. Aslam[96], K. Assamagan[30], R. Astalos[29a], K.S.V. Astrand[99], S. Atashi[164], R.J. Atkin[34a], H. Atmani[36f], P.A. Atmasiddha[130], K. Augsten[134], A.D. Auriol[41], V.A. Austrup[102], A.S. Avad[95], G. Avolio[37], K. Axiotis[56], A. Azzam[13], D. Babal[29b], H. Bachacou[137], K. Bachas[157,q], A. Bachiu[35], E. Bachmann[50], M.J. Backes[63a], A. Badea[40], T.M. Baer[107], P. Bagnaia[75a,75b], M. Bahmani[19], D. Bahner[54], K. Bai[125], J.T. Baines[136], L. Baines[95], O.K. Baker[177], E. Bakos[16], D. Bakshi Gupta[8], L.E. Balabram Filho[82b], V. Balakrishnan[122], R. Balasubramanian[4], E.M. Baldin[38], P. Balek[86a], E. Ballabene[24b,24a], F. Balli[137], L.M. Baltes[63a], W.K. Balunas[33], J. Balz[101], I. Bamwidhi[118b], E. Banas[87], M. Bandieramonte[131], A. Bandyopadhyay[25], S. Bansal[25], L. Barak[156], M. Barakat[48], E.L. Barberio[106], D. Barberis[18b], M. Barbero[103], M.Z. Barel[116], T. Barillari[111], M-S. Barisits[37], T. Barklow[148], P. Baron[135], D.A. Baron Moreno[102], A. Baroncelli[62], A.J. Barr[128], J.D. Barr[97], F. Barreiro[100], J. Barreiro Guimarães da Costa[14], M.G. Barros Teixeira[132a], S. Barsov[38], F. Bartels[63a], R. Bartoldus[148], A.E. Barton[92], P. Bartos[29a], M. Baselga[49], S. Bashiri[87], A. Bassalat[66,b], M.J. Basso[161a], S. Bataju[45], R. Bate[169], R.L. Bates[59], S. Batlamous[100], M. Battaglia[138], D. Battulga[19], M. Bauce[75a,75b], M. Bauer[79], P. Bauer[25], L.T. Bayer[48], L.T. Bazzano Hurrell[31], J.B. Beacham[111], T. Beau[129], J.Y. Beaucamp[91], P.H. Beauchemin[163], P. Bechtle[25], H.P. Beck[20,p], K. Becker[172], A.J. Beddall[81],

JHEP01(2026)117

V.A. Bednyakov[39], C.P. Bee[150], L.J. Beemster[16], M. Begalli[82d], M. Begel[30], J.K. Behr[48], J.F. Beirer[37], F. Beisiegel[25], M. Belfkir[118b], G. Bella[156], L. Bellagamba[24b], A. Bellerive[35], C.D. Bellgraph[68], P. Bellos[21], K. Beloborodov[38], I. Benaoumeur[21], D. Benchekroun[36a], F. Bendebba[36a], Y. Benhammou[156], K.C. Benkendorfer[61], L. Beresford[48], M. Beretta[53], E. Bergeaas Kuutmann[166], N. Berger[4], B. Bergmann[134], J. Beringer[18a], G. Bernardi[5], C. Bernius[148], F.U. Bernlochner[25], A. Berrocal Guardia[13], T. Berry[96], P. Berta[135], A. Berti[132a], R. Bertrand[103], S. Bethke[111], A. Betti[75a,75b], A.J. Bevan[95], L. Bezio[56], N.K. Bhalla[54], S. Bharthuar[111], S. Bhatta[150], P. Bhattarai[148], Z.M. Bhatti[119], K.D. Bhide[54], V.S. Bhopatkar[123], R.M. Bianchi[131], G. Bianco[24b,24a], O. Biebel[110], M. Biglietti[77a], C.S. Billingsley[45], Y. Bimgdi[36f], M. Bindi[55], A. Bingham[176], A. Bingul[22b], C. Bini[75a,75b], G.A. Bird[33], M. Birman[174], M. Biros[135], S. Biryukov[151], T. Bisanz[49], E. Bisceglie[24b,24a], J.P. Biswal[136], D. Biswas[146], I. Bloch[48], A. Blue[59], U. Blumenschein[95], V.S. Bobrovnikov[39], L. Boccardo[57b,57a], M. Boehler[54], B. Boehm[171], D. Bogavac[13], A.G. Bogdanchikov[38], L.S. Boggia[129], V. Boisvert[96], P. Bokan[37], T. Bold[86a], M. Bomben[5], M. Bona[95], M. Boonekamp[137], A.G. Borbély[59], I.S. Bordulev[38], G. Borissov[92], D. Bortoletto[128], D. Boscherini[24b], M. Bosman[13], K. Bouaouda[36a], N. Bouchhar[168], L. Boudet[4], J. Boudreau[131], E.V. Bouhova-Thacker[92], D. Boumediene[41], R. Bouquet[57b,57a], A. Boveia[121], J. Boyd[37], D. Boye[30], I.R. Boyko[39], L. Bozianu[56], J. Bracinik[21], N. Brahimi[4], G. Brandt[176], O. Brandt[33], B. Brau[104], J.E. Brau[125], R. Brener[174], L. Brenner[116], R. Brenner[166], S. Bressler[174], G. Brianti[78a,78b], D. Britton[59], D. Britzger[111], I. Brock[25], R. Brock[108], G. Brooijmans[42], A.J. Brooks[68], E.M. Brooks[161b], E. Brost[30], L.M. Brown[170,161a], L.E. Bruce[61], T.L. Bruckler[128], P.A. Bruckman de Renstrom[87], B. Brüers[48], A. Bruni[24b], G. Bruni[24b], D. Brunner[47a,47b], M. Bruschi[24b], N. Bruscino[75a,75b], T. Buanes[17], Q. Buat[141], D. Buchin[111], A.G. Buckley[59], O. Bulekov[81], B.A. Bullard[148], S. Burdin[93], C.D. Burgard[49], A.M. Burger[90], B. Burghgrave[8], O. Burlayenko[54], J. Burleson[167], J.C. Burzynski[147], E.L. Busch[42], V. Büscher[101], P.J. Bussey[59], O. But[25], J.M. Butler[26], C.M. Buttar[59], J.M. Butterworth[97], W. Buttinger[136], C.J. Buxo Vazquez[108], A.R. Buzykaev[39], S. Cabrera Urbán[168], L. Cadamuro[66], H. Cai[37], Y. Cai[24b,113c,24a], Y. Cai[113a], V.M.M. Cairo[37], O. Cakir[3a], N. Calace[37], P. Calafiura[18a], G. Calderini[129], P. Calfayan[35], L. Calic[99], G. Callea[59], L.P. Caloba[82b], D. Calvet[41], S. Calvet[41], R. Camacho Toro[129], S. Camarda[37], D. Camarero Munoz[27], P. Camarri[76a,76b], C. Camincher[170], M. Campanelli[97], A. Camplani[43], V. Canale[72a,72b], A.C. Canbay[3a], E. Canonero[96], J. Cantero[168], Y. Cao[167], F. Capocasa[27], M. Capua[44b,44a], A. Carbone[71a,71b], R. Cardarelli[76a], J.C.J. Cardenas[8], M.P. Cardiff[27], G. Carducci[44b,44a], T. Carli[37], G. Carlino[72a], J.I. Carlotto[13], B.T. Carlson[131,r], E.M. Carlson[170], J. Carmignani[93], L. Carminati[71a,71b], A. Carnelli[4], M. Carnesale[37], S. Caron[115], E. Carquin[139g], I.B. Carr[106], S. Carrá[73a,73b], G. Carratta[24b,24a], C. Carrion Martinez[168], A.M. Carroll[125], M.P. Casado[13,h], P. Casolaro[72a,72b], M. Caspar[48], W.R. Castiglioni[40], F.L. Castillo[4], L. Castillo Garcia[13], V. Castillo Gimenez[168], N.F. Castro[132a,132e], A. Catinaccio[37], J.R. Catmore[127], T. Cavaliere[4], V. Cavaliere[30], L.J. Caviedes Betancourt[23b], E. Celebi[81], S. Cella[37], V. Cepaitis[56], K. Cerny[124], A.S. Cerqueira[82a], A. Cerri[74a,74b,am], L. Cerrito[76a,76b], F. Cerutti[18a], B. Cervato[71a,71b],

JHEP01(2026)117

A. Cervelli[24b], G. Cesarini[53], S.A. Cetin[81], P.M. Chabrillat[129], R. Chakkappai[66], S. Chakraborty[172], A. Chambers[61], J. Chan[18a], W.Y. Chan[158], J.D. Chapman[33], E. Chapon[137], B. Chargeishvili[154b], D.G. Charlton[21], C. Chauhan[135], Y. Che[113a], S. Chekanov[6], G.A. Chelkov[39,a], B. Chen[156], B. Chen[170], H. Chen[30], J. Chen[143a], J. Chen[147], M. Chen[128], S. Chen[88], S.J. Chen[113a], X. Chen[143a], X. Chen[15,ah], Z. Chen[62], C.L. Cheng[175], H.C. Cheng[64a], S. Cheong[148], A. Cheplakov[39], E. Cherepanova[116], R. Cherkaoui El Moursli[36e], E. Cheu[7], K. Cheung[65], L. Chevalier[137], V. Chiarella[53], G. Chiarelli[74a], G. Chiodini[70a], A.S. Chisholm[21], A. Chitan[28b], M. Chitishvili[168], M.V. Chizhov[39,s], K. Choi[11], Y. Chou[141], E.Y.S. Chow[115], K.L. Chu[174], M.C. Chu[64a], X. Chu[14,113c], Z. Chubinidze[53], J. Chudoba[133], J.J. Chwastowski[87], D. Cieri[111], K.M. Ciesla[86a], V. Cindro[94], A. Ciocio[18a], F. Cirotto[72a,72b], Z.H. Citron[174], M. Citterio[71a], D.A. Ciubotaru[28b], A. Clark[56], P.J. Clark[52], N. Clarke Hall[97], C. Clarry[160], S.E. Clawson[48], C. Clement[47a,47b], L. Clissa[24b,24a], Y. Coadou[103], M. Cobal[69a,69c], A. Coccaro[57b], R.F. Coelho Barrue[132a], R. Coelho Lopes De Sa[104], S. Coelli[71a], M.M. Cohen[130], L.S. Colangeli[160], B. Cole[42], P. Collado Soto[100], J. Collot[60], R. Coluccia[70a,70b], P. Conde Muiño[132a,132g], M.P. Connell[34c], S.H. Connell[34c], E.I. Conroy[128], M. Contreras Cossio[11], F. Conventi[72a,aj], A.M. Cooper-Sarkar[128], L. Corazzina[75a,75b], F.A. Corchia[24b,24a], A. Cordeiro Oudot Choi[141], L.D. Corpe[41], M. Corradi[75a,75b], F. Corriveau[105,ab], A. Cortes-Gonzalez[158], M.J. Costa[168], F. Costanza[4], D. Costanzo[144], J. Couthures[4], G. Cowan[96], K. Cranmer[175], L. Cremer[49], D. Cremonini[24b,24a], S. Crépé-Renaudin[60], F. Crescioli[129], T. Cresta[73a,73b], M. Cristinziani[146], M. Cristoforetti[78a,78b], E. Critelli[97], V. Croft[116], G. Crosetti[44b,44a], A. Cueto[100], H. Cui[97], Z. Cui[7], B.M. Cunnett[151], W.R. Cunningham[59], F. Curcio[168], J.R. Curran[52], M.J. Da Cunha Sargedas De Sousa[57b,57a], J.V. Da Fonseca Pinto[82b], C. Da Via[102], W. Dabrowski[86a], T. Dado[37], S. Dahbi[153], T. Dai[107], D. Dal Santo[20], C. Dallapiccola[104], M. Dam[43], G. D'amen[30], V. D'Amico[110], J.R. Dandoy[35], M. D'Andrea[57b,57a], D. Dannheim[37], G. D'anniballe[74a,74b], M. Danninger[147], V. Dao[150], G. Darbo[57b], S.J. Das[30], F. Dattola[48], S. D'Auria[71a,71b], A. D'Avanzo[72a,72b], T. Davidek[135], J. Davidson[172], I. Dawson[95], K. De[8], C. De Almeida Rossi[160], R. De Asmundis[72a], N. De Biase[48], S. De Castro[24b,24a], N. De Groot[115], P. de Jong[116], H. De la Torre[117], A. De Maria[113a], A. De Salvo[75a], U. De Sanctis[76a,76b], F. De Santis[70a,70b], A. De Santo[151], J.B. De Vivie De Regie[60], J. Debevc[94], D.V. Dedovich[39], J. Degens[93], A.M. Deiana[45], J. Del Peso[100], L. Delagrange[129], F. Deliot[137], C.M. Delitzsch[49], M. Della Pietra[72a,72b], D. Della Volpe[56], A. Dell'Acqua[37], L. Dell'Asta[71a,71b], M. Delmastro[4], C.C. Delogu[57b,57a], P.A. Delsart[60], S. Demers[177], M. Demichev[39], S.P. Denisov[38], H. Denizli[22a,l], M.G. Depala[93], L. D'Eramo[41], D. Derendarz[87], F. Derue[129], P. Dervan[93,†], A.M. Desai[1], K. Desch[25], F.A. Di Bello[74a,74b], A. Di Ciaccio[76a,76b], L. Di Ciaccio[4], A. Di Domenico[75a,75b], C. Di Donato[72a,72b], A. Di Girolamo[37], G. Di Gregorio[66], A. Di Luca[78a,78b], B. Di Micco[77a,77b], R. Di Nardo[77a,77b], K.F. Di Petrillo[40], M. Diamantopoulou[35], F.A. Dias[116], M.A. Diaz[139a,139b], A.R. Didenko[39], M. Didenko[168], S.D. Diefenbacher[18a], E.B. Diehl[107], S. Díez Cornell[48], C. Diez Pardos[146], C. Dimitriadi[149], A. Dimitrievska[21], A. Dimri[150], Y. Ding[62], J. Dingfelder[25], T. Dingley[128], I-M. Dinu[28b], S.J. Dittmeier[63b],

F. Dittus[37], M. Divisek[135], B. Dixit[93], F. Djama[103], T. Djobava[154b], C. Doglioni[102,99], A. Dohnalova[29a], Z. Dolezal[135], K. Domijan[86a], K.M. Dona[40], M. Donadelli[82d], B. Dong[108], J. Donini[41], A. D'Onofrio[72a,72b], M. D'Onofrio[93], J. Dopke[136], A. Doria[72a], N. Dos Santos Fernandes[132a], I.A. Dos Santos Luz[82e], P. Dougan[102], M.T. Dova[91], A.T. Doyle[59], M.P. Drescher[55], E. Dreyer[174], I. Drivas-koulouris[10], M. Drnevich[119], D. Du[62], T.A. du Pree[116], Z. Duan[113a], M. Dubau[4], F. Dubinin[39], M. Dubovsky[29a], E. Duchovni[174], G. Duckeck[110], P.K. Duckett[97], O.A. Ducu[28b], D. Duda[52], A. Dudarev[37], M.M. Dudek[87], E.R. Duden[27], M. D'uffizi[102], L. Duflot[66], M. Dührssen[37], I. Duminica[28g], A.E. Dumitriu[28b], M. Dunford[63a], K. Dunne[47a,47b], A. Duperrin[103], H. Duran Yildiz[3a], A. Durglishvili[154b], G.I. Dyckes[18a], M. Dyndal[86a], B.S. Dziedzic[37], Z.O. Earnshaw[151], G.H. Eberwein[128], B. Eckerova[29a], S. Eggebrecht[55], E. Egidio Purcino De Souza[82e], G. Eigen[17], K. Einsweiler[18a], T. Ekelof[166], P.A. Ekman[99], S. El Farkh[36b], Y. El Ghazali[62], H. El Jarrari[105], A. El Moussaouy[36a], D. Elitez[37], M. Ellert[166], F. Ellinghaus[176], T.A. Elliot[96], N. Ellis[37], J. Elmsheuser[30], M. Elsawy[118a], M. Elsing[37], D. Emeliyanov[136], Y. Enari[83], S. Epari[109], D. Ernani Martins Neto[87], F. Ernst[37], M. Escalier[66], C. Escobar[168], E. Etzion[156], G. Evans[132a,132b], H. Evans[68], L.S. Evans[48], A. Ezhilov[38], S. Ezzarqtouni[36a], F. Fabbri[24b,24a], L. Fabbri[24b,24a], G. Facini[97], V. Fadeyev[138], R.M. Fakhrutdinov[38], D. Fakoudis[101], S. Falciano[75a], L.F. Falda Ulhoa Coelho[27], F. Fallavollita[111], G. Falsetti[44b,44a], J. Faltova[135], C. Fan[167], K.Y. Fan[64b], Y. Fan[14], Y. Fang[14,113c], M. Fanti[71a,71b], M. Faraj[69a,69b], Z. Farazpay[98], A. Farbin[8], A. Farilla[77a], K. Farman[153], T. Farooque[108], J.N. Farr[177], M.S. Farrington[61], S.M. Farrington[136,52], F. Fassi[36e], D. Fassouliotis[9], L. Fayard[66], P. Federic[135], P. Federicova[133], O.L. Fedin[38,a], M. Feickert[175], L. Feligioni[103], D.E. Fellers[18a], C. Feng[142a], Y. Feng[14], Z. Feng[116], M.J. Fenton[164], L. Ferencz[48], B. Fernandez Barbadillo[92], P. Fernandez Martinez[67], M.J.V. Fernoux[103], J. Ferrando[92], A. Ferrari[166], P. Ferrari[116,115], R. Ferrari[73a], D. Ferrere[56], C. Ferretti[107], M.P. Fewell[1], D. Fiacco[75a,75b], F. Fiedler[101], P. Fiedler[134], S. Filimonov[39], M.S. Filip[28b,t], A. Filipčič[94], E.K. Filmer[161a], F. Filthaut[115], M.C.N. Fiolhais[132a,132c,c], L. Fiorini[168], W.C. Fisher[108], T. Fitschen[102], P.M. Fitzhugh[137], I. Fleck[146], P. Fleischmann[107], T. Flick[176], M. Flores[34d,ag], L.R. Flores Castillo[64a], M. Foll[127], F.M. Follega[78a,78b], N. Fomin[33], J.H. Foo[160], A. Formica[137], A.C. Forti[102], E. Fortin[37], A.W. Fortman[18a], L. Foster[18a], L. Fountas[9,i], D. Fournier[66], H. Fox[92], P. Francavilla[74a,74b], S. Francescato[61], S. Franchellucci[56], M. Franchini[24b,24a], S. Franchino[63a], D. Francis[37], L. Franco[48], L. Franconi[48], M. Franklin[61], G. Frattari[27], Y.Y. Frid[156], J. Friend[59], N. Fritzsche[37], A. Froch[56], D. Froidevaux[37], J.A. Frost[136], Y. Fu[108], S. Fuenzalida Garrido[139g], M. Fujimoto[150], K.Y. Fung[64a], E. Furtado De Simas Filho[82e], M. Furukawa[158], M. Fuste Costa[48], J. Fuster[168], A. Gaa[55], A. Gabrielli[24b,24a], A. Gabrielli[160], P. Gadow[37], G. Gagliardi[57b,57a], L.G. Gagnon[18a], S. Gaid[84b], S. Galantzan[156], J. Gallagher[1], E.J. Gallas[128], A.L. Gallen[166], B.J. Gallop[136], K.K. Gan[121], S. Ganguly[158], Y. Gao[52], A. Garabaglu[141], F.M. Garay Walls[139a,139b], C. García[168], A. Garcia Alonso[116], A.G. Garcia Caffaro[177], J.E. García Navarro[168], M.A. Garcia Ruiz[23b], M. Garcia-Sciveres[18a], G.L. Gardner[130], R.W. Gardner[40], N. Garelli[163], R.B. Garg[148], J.M. Gargan[33], C.A. Garner[160], C.M. Garvey[34a], V.K. Gassmann[163], G. Gaudio[73a], V. Gautam[13], P. Gauzzi[75a,75b], J. Gavranovic[94], I.L. Gavrilenko[132a], A. Gavrilyuk[38], C. Gay[169], G. Gaycken[125], E.N. Gazis[10], A. Gekow[121], C. Gemme[57b], M.H. Genest[60], A.D. Gentry[114], S. George[96], T. Geralis[46], A.A. Gerwin[122], P. Gessinger-Befurt[37], M. Ghani[172], K. Ghorbanian[95], A. Ghosal[146], A. Ghosh[164], A. Ghosh[7], B. Giacobbe[24b], S. Giagu[75a,75b], T. Giani[116], A. Giannini[62], S.M. Gibson[96], M. Gignac[138], D.T. Gil[86b], A.K. Gilbert[86a], B.J. Gilbert[42], D. Gillberg[35], G. Gilles[116], D.M. Gingrich[2,ai], M.P. Giordani[69a,69c], P.F. Giraud[137], G. Giugliarelli[69a,69c], D. Giugni[71a], F. Giuli[76a,76b], I. Gkialas[9,i], L.K. Gladilin[38], C. Glasman[100], M. Glazewska[20], R.M. Gleason[164], G. Glemža[48], M. Glisic[125], I. Gnesi[44b], Y. Go[30], M. Goblirsch-Kolb[37], B. Gocke[49], D. Godin[109], B. Gokturk[22a], S. Goldfarb[106], T. Golling[56], M.G.D. Gololo[34c], A. Golub[141], D. Golubkov[38], J.P. Gombas[108], A. Gomes[132a,132b], G. Gomes Da Silva[146], A.J. Gomez Delegido[37], R. Gonçalo[132a], L. Gonella[21], A. Gongadze[154c], F. Gonnella[21], J.L. Gonski[148], R.Y. González Andana[52], S. González de la Hoz[168], M.V. Gonzalez Rodrigues[48], R. Gonzalez Suarez[166], S. Gonzalez-Sevilla[56], L. Goossens[37], B. Gorini[37], E. Gorini[70a,70b], A. Gorišek[94], T.C. Gosart[130], A.T. Goshaw[51], M.I. Gostkin[39], S. Goswami[123], C.A. Gottardo[37], S.A. Gotz[110], M. Gouighri[36b], A.G. Goussiou[141], N. Govender[34c], R.P. Grabarczyk[128], I. Grabowska-Bold[86a], K. Graham[35], E. Gramstad[127], S. Grancagnolo[70a,70b], C.M. Grant[1], P.M. Gravila[28f], F.G. Gravili[70a,70b], H.M. Gray[18a], M. Greco[111], M.J. Green[1], C. Grefe[25], A.S. Grefsrud[17], I.M. Gregor[48], K.T. Greif[164], P. Grenier[148], S.G. Grewe[111], A.A. Grillo[138], K. Grimm[32], S. Grinstein[13,x], J.-F. Grivaz[66], E. Gross[174], J. Grosse-Knetter[55], L.H. Grossman[18b], L. Guan[107], G. Guerrieri[37], R. Guevara[127], R. Gugel[101], J.A.M. Guhit[107], A. Guida[19], E. Guilloton[172], S. Guindon[37], F. Guo[14,113c], J. Guo[143a], L. Guo[48], L. Guo[113b,v], Y. Guo[107], Y. Guo[42], A. Gupta[49], R. Gupta[131], S. Gupta[27], S. Gurbuz[25], S.S. Gurdasani[48], G. Gustavino[75a,75b], P. Gutierrez[122], L.F. Gutierrez Zagazeta[130], M. Gutsche[50], C. Gutschow[97], C. Gwenlan[128], C.B. Gwilliam[93], E.S. Haaland[127], A. Haas[119], M. Habedank[59], C. Haber[18a], H.K. Hadavand[8], A. Haddad[41], A. Hadef[50], A.I. Hagan[92], J.J. Hahn[146], E.H. Haines[97], M. Haleem[171], J. Haley[123], G.D. Hallewell[103], J.A. Hallford[48], K. Hamano[170], H. Hamdaoui[166], M. Hamer[25], S.E.D. Hammoud[66], E.J. Hampshire[96], J. Han[142a], L. Han[113a], L. Han[62], S. Han[14], K. Hanagaki[83], M. Hance[138], D.A. Hangal[42], H. Hanif[147], M.D. Hank[130], J.B. Hansen[43], P.H. Hansen[43], T. Harenberg[176], S. Harkusha[178], M.L. Harris[104], Y.T. Harris[25], J. Harrison[13], P.F. Harrison[172], M.L.E. Hart[97], N.M. Hartman[111], N.M. Hartmann[110], R.Z. Hasan[96,136], Y. Hasegawa[145], F. Haslbeck[128], S. Hassan[17], R. Hauser[108], M. Haviernik[135], C.M. Hawkes[21], R.J. Hawkings[37], Y. Hayashi[158], D. Hayden[108], C. Hayes[107], R.L. Hayes[116], C.P. Hays[128], J.M. Hays[95], H.S. Hayward[93], M. He[14,113c], Y. He[48], Y. He[97], N.B. Heatley[95], V. Hedberg[99], J. Heilman[35], S. Heim[48], T. Heim[18a], J.J. Heinrich[125], L. Heinrich[111], J. Hejbal[133], M. Helbig[50], A. Held[175], S. Hellesund[17], C.M. Helling[169], S. Hellman[47a,47b], A.M. Henriques Correia[37], H. Herde[99], Y. Hernández Jiménez[150], L.M. Herrmann[25], T. Herrmann[50], G. Herten[54], R. Hertenberger[110], L. Hervas[37], M.E. Hesping[101], N.P. Hessey[161a], J. Hessler[111], M. Hidaoui[36b], N. Hidic[135], E. Hill[160], T.S. Hillersoy[17], S.J. Hillier[21], J.R. Hinds[108], F. Hinterkeuser[25], M. Hirose[126],

S. Hirose[162], D. Hirschbuehl[176], T.G. Hitchings[102], B. Hiti[94], J. Hobbs[150], R. Hobincu[28e], N. Hod[174], A.M. Hodges[167], M.C. Hodgkinson[144], B.H. Hodkinson[128], A. Hoecker[37], D.D. Hofer[107], J. Hofer[168], J. Hofner[101], M. Holzbock[37], L.B.A.H. Hommels[33], V. Homsak[128], J.J. Hong[68], T.M. Hong[131], B.H. Hooberman[167], W.H. Hopkins[6], M.C. Hoppesch[167], Y. Horii[112], M.E. Horstmann[111], S. Hou[153], M.R. Housenga[167], J. Howarth[59], J. Hoya[6], M. Hrabovsky[124], T. Hryn'ova[4], P.J. Hsu[65], S.-C. Hsu[141], T. Hsu[66], M. Hu[18a], Q. Hu[62], S. Huang[33], X. Huang[14,113c], Y. Huang[135], Y. Huang[113b], Y. Huang[14], Z. Huang[66], Z. Hubacek[134], F. Huegging[25], T.B. Huffman[128], M. Hufnagel Maranha De Faria[82a], C.A. Hugli[48], M. Huhtinen[37], S.K. Huiberts[127], R. Hulsken[105], C.E. Hultquist[18a], D.L. Humphreys[104], N. Huseynov[12], J. Huston[108], J. Huth[61], L. Huth[48], R. Hyneman[7], G. Iacobucci[56], G. Iakovidis[30], L. Iconomidou-Fayard[66], J.P. Iddon[37], P. Iengo[72a,72b], Y. Iiyama[158], T. Iizawa[158], Y. Ikegami[83], D. Iliadis[157], N. Ilic[160], H. Imam[36a], G. Inacio Goncalves[82d], S.A. Infante Cabanas[139c], T. Ingebretsen Carlson[47a,47b], J.M. Inglis[95], G. Introzzi[73a,73b], M. Iodice[77a], V. Ippolito[75a,75b], R.K. Irwin[93], M. Ishino[158], W. Islam[175], C. Issever[19], S. Istin[22a,ao], K. Itabashi[126], H. Ito[173], R. Iuppa[78a,78b], A. Ivina[174], S. Izumiyama[112], V. Izzo[72a], P. Jacka[134], P. Jackson[1], P. Jain[48], K. Jakobs[54], T. Jakoubek[174], J. Jamieson[59], W. Jang[158], S. Jankovych[135], M. Javurkova[104], P. Jawahar[102], L. Jeanty[125], J. Jejelava[154a,ae], P. Jenni[54,f], C.E. Jessiman[35], C. Jia[142a], H. Jia[169], J. Jia[150], X. Jia[111,113c], Z. Jia[113a], C. Jiang[52], Q. Jiang[64b], S. Jiggins[48], M. Jimenez Ortega[168], J. Jimenez Pena[13], S. Jin[113a], A. Jinaru[28b], O. Jinnouchi[140], P. Johansson[144], K.A. Johns[7], J.W. Johnson[138], F.A. Jolly[48], D.M. Jones[151], E. Jones[48], K.S. Jones[8], P. Jones[33], R.W.L. Jones[92], T.J. Jones[93], H.L. Joos[55], R. Joshi[121], J. Jovicevic[16], X. Ju[18a], J.J. Junggeburth[37], T. Junkermann[63a], A. Juste Rozas[13,x], M.K. Juzek[87], S. Kabana[139f], A. Kaczmarska[87], S.A. Kadir[148], M. Kado[111], H. Kagan[121], M. Kagan[148], A. Kahn[130], C. Kahra[101], T. Kaji[158], E. Kajomovitz[155], N. Kakati[174], N. Kakoty[13], I. Kalaitzidou[54], S. Kandel[8], N. Kanellos[10], N.J. Kang[138], D. Kar[34j], E. Karentzos[25], K. Karki[8], O. Karkout[116], S.N. Karpov[39], Z.M. Karpova[39], V. Kartvelishvili[92,154b], A.N. Karyukhin[38], E. Kasimi[157], J. Katzy[48], S. Kaur[35], K. Kawade[145], M.P. Kawale[122], C. Kawamoto[88], T. Kawamoto[62], E.F. Kay[37], S. Kazakos[108], V.F. Kazanin[38], J.M. Keaveney[34a], R. Keeler[170], G.V. Kehris[61], J.S. Keller[35], J.M. Kelly[170], J.J. Kempster[151], O. Kepka[133], J. Kerr[161b], B.P. Kerridge[136], B.P. Kerševan[94], L. Keszeghova[29a], R.A. Khan[131], A. Khanov[123], A.G. Kharlamov[38], T. Kharlamova[38], E.E. Khoda[141], M. Kholodenko[132a], T.J. Khoo[19], G. Khoriauli[171], Y. Khoulaki[36a], Y.A.R. Khwaira[129], B. Kibirige[34j], D. Kim[6], D.W. Kim[18b], Y.K. Kim[40], N. Kimura[97], M.K. Kingston[55], A. Kirchhoff[55], C. Kirfel[25], F. Kirfel[25], J. Kirk[136], A.E. Kiryunin[111], S. Kita[162], O. Kivernyk[25], M. Klassen[163], C. Klein[35], L. Klein[171], M.H. Klein[45], S.B. Klein[56], U. Klein[93], A. Klimentov[30], T. Klioutchnikova[37], P. Kluit[116], S. Kluth[111], E. Kneringer[79], T.M. Knight[160], A. Knue[49], M. Kobel[50], D. Kobylianskii[174], S.F. Koch[128], M. Kocian[148], P. Kodyš[135], D.M. Koeck[125], T. Koffas[35], O. Kolay[50], I. Koletsou[4], T. Komarek[87], K. Köneke[55], A.X.Y. Kong[1], T. Kono[120], N. Konstantinidis[97], P. Kontaxakis[56], B. Konya[99], R. Kopeliansky[42], S. Koperny[86a], R. Koppenhofer[54], K. Korcyl[87], K. Kordas[157,d],

JHEP01(2026)117

A. Korn[97], S. Korn[55], I. Korolkov[13], N. Korotkova[38], B. Kortman[116], O. Kortner[111], S. Kortner[111], W.H. Kostecka[117], M. Kostov[29a], V.V. Kostyukhin[146], A. Kotsokechagia[37], A. Kotwal[51], A. Koulouris[37], A. Kourkoumeli-Charalampidi[73a,73b], C. Kourkoumelis[9], E. Kourlitis[111], O. Kovanda[125], R. Kowalewski[170], W. Kozanecki[125], A.S. Kozhin[38], V.A. Kramarenko[38], G. Kramberger[94], P. Kramer[25], M.W. Krasny[129], A. Krasznahorkay[104], A.C. Kraus[117], J.W. Kraus[176], J.A. Kremer[48], N.B. Krengel[146], T. Kresse[50], L. Kretschmann[176], J. Kretzschmar[93], P. Krieger[160], K. Krizka[21], K. Kroeninger[49], H. Kroha[111], J. Kroll[133], J. Kroll[130], K.S. Krowpman[108], U. Kruchonak[39], H. Krüger[25], N. Krumnack[80], M.C. Kruse[51], O. Kuchinskaia[39], S. Kuday[3a], S. Kuehn[37], R. Kuesters[54], T. Kuhl[48], V. Kukhtin[39], Y. Kulchitsky[39], S. Kuleshov[139d,139b], J. Kull[1], E.V. Kumar[110], M. Kumar[34j], N. Kumari[48], P. Kumari[161b], A. Kupco[133], A. Kupich[38], O. Kuprash[54], H. Kurashige[85], L.L. Kurchaninov[161a], O. Kurdysh[4], A. Kurova[38], M. Kuze[140], A.K. Kvam[104], J. Kvita[124], N.G. Kyriacou[141], M. Laassiri[30], C. Lacasta[168], F. Lacava[75a,75b], H. Lacker[19], D. Lacour[129], N.N. Lad[97], E. Ladygin[39], A. Lafarge[41], B. Laforge[129], T. Lagouri[177], F.Z. Lahbabi[36a], S. Lai[55,37], W.S. Lai[97], I.K. Lakomiec[55], J.E. Lambert[170], S. Lammers[68], W. Lampl[7], C. Lampoudis[157,d], G. Lamprinoudis[171], A.N. Lancaster[117], E. Lançon[30], U. Landgraf[54], M.P.J. Landon[95], V.S. Lang[54], A.J. Lankford[164], F. Lanni[37], C.S. Lantz[167], K. Lantzsch[25], A. Lanza[73a], M. Lanzac Berrocal[168], J.F. Laporte[137], T. Lari[71a], D. Larsen[17], L. Larson[11], F. Lasagni Manghi[24b], M. Lassnig[37], S.D. Lawlor[144], R. Lazaridou[164], M. Lazzaroni[71a,71b], E.T.T. Le[164], H.D.M. Le[108], E.M. Le Boulicaut[177], L.T. Le Pottier[18a], B. Leban[24b,24a], F. Ledroit-Guillon[60], T.F. Lee[161b], L.L. Leeuw[34c], M. Lefebvre[170], C. Leggett[18a], G. Lehmann Miotto[37], M. Leigh[56], W.A. Leight[104], W. Leinonen[115], A. Leisos[157,u], M.A.L. Leite[82c], C.E. Leitgeb[19], R. Leitner[135], K.J.C. Leney[45], T. Lenz[25], S. Leone[74a], C. Leonidopoulos[52], A. Leopold[149], J.H. Lepage Bourbonnais[35], R. Les[108], C.G. Lester[33], M. Levchenko[38], J. Levêque[4], L.J. Levinson[174], G. Levrini[24b,24a], M.P. Lewicki[87], C. Lewis[141], D.J. Lewis[4], L. Lewitt[144], A. Li[30], B. Li[142a], C. Li[107], C-Q. Li[111], H. Li[142a], H. Li[102], H. Li[15], H. Li[62], H. Li[142a], J. Li[143a], K. Li[14], L. Li[143a], R. Li[177], S. Li[14,113c], S. Li[143b,143a], T. Li[5], X. Li[105], Y. Li[14], Z. Li[158], Z. Li[14,113c], Z. Li[62], S. Liang[14,113c], Z. Liang[14], M. Liberatore[137], B. Liberti[76a], G.B. Libotte[82d], K. Lie[64c], J. Lieber Marin[82e], H. Lien[68], H. Lin[107], S.F. Lin[150], L. Linden[110], R.E. Lindley[7], J.H. Lindon[37], J. Ling[61], E. Lipeles[130], A. Lipniacka[17], A. Lister[169], J.D. Little[68], B. Liu[14], B.X. Liu[113b], D. Liu[155], D. Liu[138], E.H.L. Liu[21], J.K.K. Liu[119], K. Liu[143b], K. Liu[143b,143a], M. Liu[62], M.Y. Liu[62], P. Liu[14], Q. Liu[148], S. Liu[150], X. Liu[142a], Y. Liu[113b,113c], Y. Liu[167], Y.L. Liu[142a], Y.W. Liu[62], Z. Liu[66,k], S.L. Lloyd[95], E.M. Lobodzinska[48], P. Loch[7], E. Lodhi[160], K. Lohwasser[144], E. Loiacono[48], J.D. Lomas[21], J.D. Long[42], I. Longarini[164], R. Longo[167], A. Lopez Solis[13], N.A. Lopez-canelas[7], N. Lorenzo Martinez[4], A.M. Lory[110], M. Losada[118a], G. Löschcke Centeno[4], X. Lou[47a,47b], X. Lou[14,113c], A. Lounis[66], P.A. Love[92], M. Lu[66], S. Lu[130], Y.J. Lu[153], H.J. Lubatti[141], C. Luci[75a,75b], F.L. Lucio Alves[113a], F. Luehring[68], B.S. Lunday[130], O. Lundberg[149], J. Lunde[37], N.A. Luongo[6], M.S. Lutz[37], A.B. Lux[26], D. Lynn[30], R. Lysak[133], V. Lysenko[134], E. Lytken[99], V. Lyubushkin[39],

JHEP01(2026)117

T. Lyubushkina[39], M.M. Lyukova[150], H. Ma[30], K. Ma[62], L.L. Ma[142a], W. Ma[62], Y. Ma[123], J.C. MacDonald[101], P.C. Machado De Abreu Farias[82e], D. Macina[37], R. Madar[41], T. Madula[97], J. Maeda[85], T. Maeno[30], P.T. Mafa[34c,j], H. Maguire[144], M. Maheshwari[33], V. Maiboroda[66], A. Maio[132a,132b,132d], K. Maj[86a], O. Majersky[48], S. Majewski[125], R. Makhmanazarov[38], N. Makovec[66], V. Maksimovic[16], B. Malaescu[129], J. Malamant[127], Pa. Malecki[87], V.P. Maleev[38], F. Malek[60,o], M. Mali[94], D. Malito[96], A. Maloizel[5], S. Maltezos[10], A. Malvezzi Lopes[82d], S. Malyukov[39], J. Mamuzic[94], G. Mancini[53], M.N. Mancini[27], G. Manco[73a,73b], J.P. Mandalia[95], S.S. Mandarry[151], I. Mandić[94], L. Manhaes de Andrade Filho[82a], I.M. Maniatis[174], J. Manjarres Ramos[90], D.C. Mankad[174], A. Mann[110], T. Manoussos[37], M.N. Mantinan[40], S. Manzoni[37], L. Mao[143a], X. Mapekula[34c], A. Marantis[157], R.R. Marcelo Gregorio[95], G. Marchiori[5], C. Marcon[71a], E. Maricic[16], M. Marinescu[48], S. Marium[48], M. Marjanovic[122], A. Markhoos[54], M. Markovitch[66], M.K. Maroun[104], M.C. Marr[147], G.T. Marsden[102], E.J. Marshall[92], Z. Marshall[18a], S. Marti-Garcia[168], J. Martin[97], T.A. Martin[136], V.J. Martin[52], B. Martin dit Latour[17], L. Martinelli[75a,75b], M. Martinez[13,x], P. Martinez Agullo[168], V.I. Martinez Outschoorn[104], P. Martinez Suarez[37], S. Martin-Haugh[136], G. Martinovicova[135], V.S. Martoiu[28b], A.C. Martyniuk[97], A. Marzin[37], D. Mascione[78a,78b], L. Masetti[101], J. Masik[102], A.L. Maslennikov[39], S.L. Mason[42], P. Massarotti[72a,72b], P. Mastrandrea[74a,74b], A. Mastroberardino[44b,44a], T. Masubuchi[126], T.T. Mathew[125], J. Matousek[135], D.M. Mattern[49], K. Mauer[48], J. Maurer[28b], T. Maurin[59], A.J. Maury[66], B. Maček[94], C. Mavungu Tsava[103], D.A. Maximov[38], A.E. May[102], E. Mayer[41], R. Mazini[34j], I. Maznas[117], S.M. Mazza[138], E. Mazzeo[37], J.P. Mc Gowan[170], S.P. Mc Kee[107], C.A. Mc Lean[6], C.C. McCracken[169], E.F. McDonald[106], A.E. McDougall[116], L.F. Mcelhinney[92], J.A. Mcfayden[151], R.P. McGovern[130], R.P. Mckenzie[34j], T.C. Mclachlan[48], D.J. Mclaughlin[97], S.J. McMahon[136], C.M. Mcpartland[93], R.A. McPherson[170,ab], S. Mehlhase[110], A. Mehta[93], D. Melini[168], B.R. Mellado Garcia[34j], A.H. Melo[55], F. Meloni[48], A.M. Mendes Jacques Da Costa[102], L. Meng[92], S. Menke[111], M. Mentink[37], E. Meoni[44b,44a], G. Mercado[117], S. Merianos[157], C. Merlassino[69a,69c], C. Meroni[71a,71b], J. Metcalfe[6], A.S. Mete[6], E. Meuser[101], C. Meyer[68], J-P. Meyer[137], Y. Miao[113a], R.P. Middleton[136], M. Mihovilovic[66], L. Mijović[52], G. Mikenberg[174], M. Mikestikova[133], M. Mikuž[94], H. Mildner[101], A. Milic[37], D.W. Miller[40], E.H. Miller[148], A. Milov[174], D.A. Milstead[47a,47b], T. Min[113a], A.A. Minaenko[38], I.A. Minashvili[154b], A.I. Mincer[119], B. Mindur[86a], M. Mineev[39], Y. Mino[88], L.M. Mir[13], M. Miralles Lopez[59], M. Mironova[18a], M. Missio[41], A. Mitra[172], V.A. Mitsou[168], Y. Mitsumori[112], O. Miu[160], P.S. Miyagawa[95], T. Mkrtchyan[37], M. Mlinarevic[97], T. Mlinarevic[97], M. Mlynarikova[135], L. Mlynarska[86a], C. Mo[143a], S. Mobius[20], M.H. Mohamed Farook[114], S. Mohapatra[42], M.F. Mohd Soberi[52], S. Mohiuddin[123], G. Mokgatitswane[34j], L. Moleri[174], U. Molinatti[128], L.G. Mollier[20], B. Mondal[133], S. Mondal[134], K. Mönig[48], E. Monnier[103], L. Monsonis Romero[168], J. Montejo Berlingen[13], A. Montella[47a,47b], M. Montella[121], F. Montereali[77a,77b], F. Monticelli[91], S. Monzani[69a,69c], A. Morancho Tarda[43], N. Morange[66], A.L. Moreira De Carvalho[48], M. Moreno Llácer[168], C. Moreno Martinez[56], J.M. Moreno Perez[23b], P. Morettini[57b], S. Morgenstern[37], M. Morii[61], M. Morinaga[158],

M. Moritsu[89], F. Morodei[75a,75b], P. Moschovakos[37], B. Moser[54], M. Mosidze[154b], T. Moskalets[45], P. Moskvitina[115], J. Moss[32], P. Moszkowicz[86a], T. Motta Quirino[82d], A. Moussa[36d], Y. Moyal[174], H. Moyano Gomez[13], E.J.W. Moyse[104], T.G. Mroz[87], S. Muanza[103], M. Mucha[25], J. Mueller[131], R. Müller[37], G.A. Mullier[166], A.J. Mullin[33], J.J. Mullin[51], A.C. Mullins[45], A.E. Mulski[61], D.P. Mungo[160], D. Munoz Perez[168], F.J. Munoz Sanchez[102], W.J. Murray[172,136], M. Muškinja[94], C. Mwewa[48], A.G. Myagkov[38,a], A.J. Myers[8], G. Myers[107], M. Myska[134], B.P. Nachman[148], K. Nagai[128], K. Nagano[83], R. Nagasaka[158], J.L. Nagle[30,al], E. Nagy[103], A.M. Nairz[37], Y. Nakahama[83], K. Nakamura[83], K. Nakkalil[5], A. Nandi[63b], H. Nanjo[126], E.A. Narayanan[45], Y. Narukawa[158], I. Naryshkin[38], L. Nasella[71a,71b], S. Nasri[118b], C. Nass[25], G. Navarro[23a], A. Nayaz[19], P.Y. Nechaeva[38], S. Nechaeva[24b,24a], F. Nechansky[133], L. Nedic[128], T.J. Neep[21], A. Negri[73a,73b], M. Negrini[24b], C. Nellist[116], C. Nelson[105], K. Nelson[107], S. Nemecek[133], M. Nessi[37,g], M.S. Neubauer[167], J. Newell[93], P.R. Newman[21], Y.W.Y. Ng[167], B. Ngair[118a], H.D.N. Nguyen[109], J.D. Nichols[122], R.B. Nickerson[128], R. Nicolaidou[137], J. Nielsen[138], M. Niemeyer[55], J. Niermann[37], N. Nikiforou[37], V. Nikolaenko[38,a], I. Nikolic-Audit[129], P. Nilsson[30], I. Ninca[48], G. Ninio[156], A. Nisati[75a], R. Nisius[111], N. Nitika[174], E.K. Nkadimeng[34b], T. Nobe[158], D. Noll[148], T. Nommensen[152], M.B. Norfolk[144], B.J. Norman[35], L.C. Nosler[18a], M. Noury[36a], J. Novak[94], T. Novak[94], P. Novotny[174], R. Novotny[134], L. Nozka[124], K. Ntekas[164], D. Ntounis[148], N.M.J. Nunes De Moura Junior[82b], J. Ocariz[129], I. Ochoa[132a], A. Odella Rodriguez[13], S. Oerdek[48,y], J.T. Offermann[40], A. Ogrodnik[87], A. Oh[102], C.C. Ohm[149], H. Oide[83], M.L. Ojeda[37], Y. Okumura[158], L.F. Oleiro Seabra[132a], I. Oleksiyuk[56], G. Oliveira Correa[13], D. Oliveira Damazio[30], J.L. Oliver[1], R. Omar[68], Ö.O. Öncel[54], A.P. O'Neill[20], A. Onofre[132a,132e,e], P.U.E. Onyisi[11], M.J. Oreglia[40], D. Orestano[77a,77b], R. Orlandini[77a,77b], R.S. Orr[160], L.M. Osojnak[42], Y. Osumi[112], G. Otero y Garzon[31], H. Otono[89], M. Ouchrif[36d], F. Ould-Saada[127], T. Ovsiannikova[141], M. Owen[59], R.E. Owen[136], V.E. Ozcan[22a], F. Ozturk[87], N. Ozturk[8], S. Ozturk[81], H.A. Pacey[128], K. Pachal[161a], A. Pacheco Pages[13], C. Padilla Aranda[13], G. Padovano[75a,75b], S. Pagan Griso[18a], J. Pampel[25], J. Pan[177], D.K. Panchal[11], C.E. Pandini[60], J.G. Panduro Vazquez[136], H.D. Pandya[1], H. Pang[137], P. Pani[48], G. Panizzo[69a,69c], L. Panwar[129], L. Paolozzi[56], S. Parajuli[167], A. Paramonov[6], C. Paraskevopoulos[53], D. Paredes Hernandez[64b], S.R. Paredes Saenz[52], A. Pareti[73a,73b], K.R. Park[42], T.H. Park[111], F. Parodi[57b,57a], J.A. Parsons[42], U. Parzefall[54], B. Pascual Dias[41], L. Pascual Dominguez[100], E. Pasqualucci[75a], S. Passaggio[57b], F. Pastore[96], P. Patel[87], U.M. Patel[51], J.R. Pater[102], T. Pauly[37], F. Pauwels[135], C.I. Pazos[163], M. Pedersen[127], R. Pedro[132a], S.V. Peleganchuk[38], O. Penc[133], S. Peng[15], G.D. Penn[177], K.E. Penski[110], M. Penzin[38], B.S. Peralva[82d], A.P. Pereira Peixoto[141], L. Pereira Sanchez[148], D.V. Perepelitsa[30,al], G. Perera[104], E. Perez Codina[37], M. Perganti[10], H. Pernegger[37], S. Perrella[75a,75b], K. Peters[48], R.F.Y. Peters[102], B.A. Petersen[37], T.C. Petersen[43], E. Petit[103], V. Petousis[134], A.R. Petri[71a,71b], C. Petridou[157,d], T. Petru[135], M. Pettee[18a], A. Petukhov[81], K. Petukhova[37], R. Pezoa[139g], L. Pezzotti[24b,24a], G. Pezzullo[177], L. Pfaffenbichler[37], A.J. Pfleger[79], T.M. Pham[175], T. Pham[106], P.W. Phillips[136], G. Piacquadio[150], E. Pianori[18a],

F. Piazza[125], R. Piegaia[31], D. Pietreanu[28b], A.D. Pilkington[102], M. Pinamonti[69a,69c], J.L. Pinfold[2], G. Pinheiro Matos[42], B.C. Pinheiro Pereira[132a], J. Pinol Bel[13], A.E. Pinto Pinoargote[129], L. Pintucci[69a,69c], K.M. Piper[151], A. Pirttikoski[56], D.A. Pizzi[35], L. Pizzimento[64b], A. Plebani[33], M.-A. Pleier[30], V. Pleskot[135], E. Plotnikova[39], G. Poddar[95], R. Poettgen[99], L. Poggioli[129], S. Polacek[135], G. Polesello[73a], A. Poley[147], A. Polini[24b], C.S. Pollard[172], Z.B. Pollock[121], E. Pompa Pacchi[122], N.I. Pond[97], D. Ponomarenko[68], L. Pontecorvo[37], S. Popa[28a], G.A. Popeneciu[28d], A. Poreba[37], D.M. Portillo Quintero[161a], S. Pospisil[134], M.A. Postill[144], P. Postolache[28c], K. Potamianos[172], P.A. Potepa[86a], I.N. Potrap[39], C.J. Potter[33], H. Potti[152], J. Poveda[168], M.E. Pozo Astigarraga[37], R. Pozzi[37], A. Prades Ibanez[76a,76b], S.R. Pradhan[144], J. Pretel[170], D. Price[102], M. Primavera[70a], L. Primomo[69a,69c], M.A. Principe Martin[100], R. Privara[124], T. Procter[86b], M.L. Proffitt[141], N. Proklova[130], K. Prokofiev[64c], G. Proto[111], J. Proudfoot[6], M. Przybycien[86a], W.W. Przygoda[86b], A. Psallidas[46], J.E. Puddefoot[144], D. Pudzha[53], H.I. Purnell[1], D. Pyatiizbyantseva[115], J. Qian[107], R. Qian[108], D. Qichen[128], Y. Qin[13], T. Qiu[52], A. Quadt[55], M. Queitsch-Maitland[102], G. Quetant[56], R.P. Quinn[169], G. Rabanal Bolanos[61], D. Rafanoharana[111], F. Raffaeli[76a,76b], F. Ragusa[71a,71b], J.L. Rainbolt[40], S. Rajagopalan[30], E. Ramakoti[39], L. Rambelli[57b,57a], I.A. Ramirez-Berend[35], K. Ran[107,113c], D.S. Rankin[130], N.P. Rapheeha[34j], H. Rasheed[28b], A. Rastogi[18a], S. Rave[101], S. Ravera[57b,57a], B. Ravina[37], I. Ravinovich[174], M. Raymond[37], A.L. Read[127], N.P. Readioff[144], D.M. Rebuzzi[73a,73b], A.S. Reed[59], K. Reeves[27], D. Reikher[37], A. Rej[49], C. Rembser[37], H. Ren[62], M. Renda[28b], F. Renner[48], A.G. Rennie[59], M. Repik[56], A.L. Rescia[57b,57a], S. Resconi[71a], M. Ressegotti[57b,57a], S. Rettie[116], W.F. Rettie[35], M.M. Revering[33], E. Reynolds[18a], O.L. Rezanova[39], P. Reznicek[135], H. Riani[36d], N. Ribaric[51], B. Ricci[69a,69c], E. Ricci[78a,78b], R. Richter[111], S. Richter[47a,47b], E. Richter-Was[86b], M. Ridel[129], S. Ridouani[36d], P. Rieck[119], P. Riedler[37], E.M. Riefel[47a,47b], J.O. Rieger[116], M. Rijssenbeek[150], M. Rimoldi[34c], L. Rinaldi[24b,24a], P. Rincke[166,55], G. Ripellino[166], I. Riu[13], J.C. Rivera Vergara[170], F. Rizatdinova[123], E. Rizvi[95], B.R. Roberts[40], S.S. Roberts[138], D. Robinson[33], A. Robson[59], A. Rocchi[76a,76b], C. Roda[74a,74b], F.A. Rodriguez[117], S. Rodriguez Bosca[37], Y. Rodriguez Garcia[23a], A.M. Rodríguez Vera[117], S. Roe[37], J.T. Roemer[37], O. Røhne[127], R.A. Rojas[37], C.P.A. Roland[129], A. Romaniouk[79], E. Romano[73a,73b], M. Romano[24b], A.C. Romero Hernandez[167], N. Rompotis[93], L. Roos[129], S. Rosati[75a], B.J. Rosser[40], E. Rossi[128], E. Rossi[72a,72b], L.P. Rossi[61], L. Rossini[54], R. Rosten[121], M. Rotaru[28b], D. Rousseau[66], D. Rousso[48], S. Roy-Garand[160], A. Rozanov[103], Z.M.A. Rozario[59], Y. Rozen[155], A. Rubio Jimenez[168], V.H. Ruelas Rivera[19], T.A. Ruggeri[1], A. Ruggiero[128], A. Ruiz-Martinez[168], A. Rummler[37], G.B. Rupnik Boero[37], Z. Rurikova[54], N.A. Rusakovich[39], S. Ruscelli[49], H.L. Russell[170], G. Russo[75a,75b], J.P. Rutherfoord[7], S. Rutherford Colmenares[33], M. Rybar[135], P. Rybczynski[86a], A. Ryzhov[45], H.F-W. Sadrozinski[138], F. Safai Tehrani[75a], S. Saha[1], M. Sahinsoy[81], B. Sahoo[174], A. Saibel[168], B.T. Saifuddin[122], M. Saimpert[137], G.T. Saito[82c], M. Saito[158], T. Saito[158], A. Sala[71a,71b], A. Salnikov[148], J. Salt[168], A. Salvador Salas[156], F. Salvatore[151], A. Salzburger[37], D. Sammel[54], E. Sampson[92], D. Sampsonidis[157,d], D. Sampsonidou[125], M.A.A. Samy[59], J. Sánchez[168],

V. Sanchez Sebastian[168], H. Sandaker[127], C.O. Sander[48], J.A. Sandesara[175], M. Sandhoff[176], C. Sandoval[23b], L. Sanfilippo[63a], D.P.C. Sankey[136], T. Sano[88], A. Sansoni[53], M. Santana Queiroz[18b], L. Santi[37], C. Santoni[41], H. Santos[132a,132b], A. Santra[174], E. Sanzani[24b,24a], K.A. Saoucha[84b], J.G. Saraiva[132a,132d], J. Sardain[7], O. Sasaki[83], K. Sato[162], C. Sauer[37], E. Sauvan[4], P. Savard[160,ai], R. Sawada[158], C. Sawyer[136], L. Sawyer[98], A.M. Sayed[27], C. Sbarra[24b], A. Sbrizzi[24b,24a], T. Scanlon[97], J. Schaarschmidt[141], U. Schäfer[101], A.C. Schaffer[66,45], D. Schaile[110], R.D. Schamberger[150], C. Scharf[19], M.M. Schefer[20], V.A. Schegelsky[38], D. Scheirich[135], M. Schernau[139f], C. Scheulen[56], C. Schiavi[57b,57a], M. Schioppa[44b,44a], B. Schlag[148], S. Schlenker[37], J. Schmeing[176], E. Schmidt[111], M.A. Schmidt[176], K. Schmieden[25], C. Schmitt[101], N. Schmitt[101], S. Schmitt[48], N.A. Schneider[110], L. Schoeffel[137], A. Schoening[63b], P.G. Scholer[35], E. Schopf[146], M. Schott[25], S. Schramm[56], T. Schroer[56], H-C. Schultz-Coulon[63a], M. Schumacher[54], B.A. Schumm[138], Ph. Schune[137], H.R. Schwartz[7], A. Schwartzman[148], T.A. Schwarz[107], Ph. Schwemling[137], R. Schwienhorst[108], F.G. Sciacca[20], A. Sciandra[30], G. Sciolla[27], F. Scuri[74a], C.D. Sebastiani[37], K. Sedlaczek[117], S.C. Seidel[114], A. Seiden[138], B.D. Seidlitz[42], C. Seitz[48], J.M. Seixas[82b], G. Sekhniaidze[72a], L. Selem[60], N. Semprini-Cesari[24b,24a], A. Semushin[178], D. Sengupta[56], V. Senthilkumar[168], L. Serin[66], M. Sessa[72a,72b], H. Severini[122], F. Sforza[57b,57a], A. Sfyrla[56], Q. Sha[14], H. Shaddix[117], A.H. Shah[33], R. Shaheen[149], J.D. Shahinian[130], M. Shamim[37], L.Y. Shan[14], M. Shapiro[18a], A. Sharma[37], A.S. Sharma[169], P. Sharma[30], P.B. Shatalov[38], K. Shaw[151], S.M. Shaw[102], Q. Shen[14], D.J. Sheppard[147], P. Sherwood[97], L. Shi[97], X. Shi[14], S. Shimizu[83], I.P.J. Shipsey[128,†], S. Shirabe[89], M. Shiyakova[39,z], M.J. Shochet[40], D.R. Shope[127], B. Shrestha[122], S. Shrestha[121,an], I. Shreyber[39], M.J. Shroff[170], P. Sicho[133], A.M. Sickles[167], E. Sideras Haddad[34j,165], A.C. Sidley[116], A. Sidoti[24b], F. Siegert[50], Dj. Sijacki[16], F. Sili[62], J.M. Silva[52], I. Silva Ferreira[82b], M.V. Silva Oliveira[30], S.B. Silverstein[47a], S. Simion[66], R. Simoniello[37], E.L. Simpson[102], H. Simpson[151], L.R. Simpson[6], S. Simsek[81], S. Sindhu[55], P. Sinervo[160], S.N. Singh[27], S. Singh[30], S. Sinha[48], S. Sinha[102], M. Sioli[24b,24a], K. Sioulas[9], I. Siral[37], E. Sitnikova[48], J. Sjölin[47a,47b], A. Skaf[55], E. Skorda[21], P. Skubic[122], M. Slawinska[87], I. Slazyk[17], I. Sliusar[127], V. Smakhtin[174], B.H. Smart[136], S.Yu. Smirnov[139b], Y. Smirnov[34c], L.N. Smirnova[38,a], O. Smirnova[99], A.C. Smith[42], D.R. Smith[164], J.L. Smith[102], M.B. Smith[35], R. Smith[148], H. Smitmanns[101], M. Smizanska[92], K. Smolek[134], P. Smolyanskiy[134], A.A. Snesarev[39], H.L. Snoek[116], R.M. Snyder[51], S. Snyder[30], R. Sobie[170,ab], A. Soffer[156], C.A. Solans Sanchez[37], E.Yu. Soldatov[39], U. Soldevila[168], A.A. Solodkov[34j], S. Solomon[27], A. Soloshenko[39], K. Solovieva[54], O.V. Solovyanov[41], P. Sommer[50], A. Sonay[13], A. Sopczak[134], A.L. Sopio[52], F. Sopkova[29b], J.D. Sorenson[114], I.R. Sotarriva Alvarez[140], V. Sothilingam[63a], O.J. Soto Sandoval[139c,139b], S. Sottocornola[68], R. Soualah[84a], Z. Soumaimi[36e], D. South[48], N. Soybelman[174], S. Spagnolo[70a,70b], D. Sperlich[54], B. Spisso[72a,72b], D.P. Spiteri[59], L. Splendori[103], M. Spousta[135], E.J. Staats[35], R. Stamen[63a], E. Stanecka[87], W. Stanek-Maslouska[48], M.V. Stange[50], B. Stanislaus[18a], M.M. Stanitzki[48], E.A. Starchenko[38], G.H. Stark[138], J. Stark[90], P. Staroba[133], P. Starovoitov[84b], R. Staszewski[87], C. Stauch[110], G. Stavropoulos[46],

A. Stefl[37], A. Stein[101], P. Steinberg[30], B. Stelzer[147,161a], H.J. Stelzer[131], O. Stelzer[161a], H. Stenzel[58], T.J. Stevenson[151], G.A. Stewart[37], J.R. Stewart[123], G. Stoicea[28b], M. Stolarski[132a], S. Stonjek[111], A. Straessner[50], J. Strandberg[149], S. Strandberg[47a,47b], M. Stratmann[176], M. Strauss[122], T. Strebler[103], P. Strizenec[29b], R. Ströhmer[171], D.M. Strom[125], R. Stroynowski[45], A. Strubig[47a,47b], S.A. Stucci[30], B. Stugu[17], J. Stupak[122], N.A. Styles[48], D. Su[148], S. Su[62], X. Su[62], D. Suchy[29a], A.D. Sudhakar Ponnu[55], K. Sugizaki[130], V.V. Sulin[38], D.M.S. Sultan[128], L. Sultanaliyeva[25], S. Sultansoy[3b], S. Sun[175], W. Sun[14], N. Sur[99], N. Suri Jr[177], M.R. Sutton[151], M. Svatos[133], P.N. Swallow[33], M. Swiatlowski[161a], A. Swoboda[37], I. Sykora[29a], M. Sykora[135], T. Sykora[135], D. Ta[101], K. Tackmann[48,y], A. Taffard[164], R. Tafirout[161a], Y. Takubo[83], M. Talby[103], A.A. Talyshev[38], K.C. Tam[64b], N.M. Tamir[156], A. Tanaka[158], J. Tanaka[158], R. Tanaka[66], M. Tanasini[150], Z. Tao[169], S. Tapia Araya[139g], S. Tapprogge[101], A. Tarek Abouelfadl Mohamed[37], S. Tarem[155], K. Tariq[14], G. Tarna[37], G.F. Tartarelli[71a], M.J. Tartarin[90], P. Tas[135], M. Tasevsky[133], E. Tassi[44b,44a], A.C. Tate[167], Y. Tayalati[36e,aa], G.N. Taylor[106], W. Taylor[161b], R.J. Taylor Vara[168], A.S. Tegetmeier[90], P. Teixeira-Dias[96], J.J. Teoh[160], K. Terashi[158], J. Terron[100], S. Terzo[13], M. Testa[53], R.J. Teuscher[160,ab], A. Thaler[79], O. Theiner[56], T. Theveneaux-Pelzer[103], D.W. Thomas[96], J.P. Thomas[21], E.A. Thompson[18a], P.D. Thompson[21], E. Thomson[130], R.E. Thornberry[45], C. Tian[62], Y. Tian[56], V. Tikhomirov[81], Yu.A. Tikhonov[39], S. Timoshenko[38], D. Timoshyn[135], E.X.L. Ting[1], P. Tipton[177], A. Tishelman-Charny[30], K. Todome[140], S. Todorova-Nova[135], L. Toffolin[69a,69c], M. Togawa[83], J. Tojo[89], S. Tokár[29a], O. Toldaiev[68], G. Tolkachev[103], M. Tomoto[83], L. Tompkins[148,n], E. Torrence[125], H. Torres[90], D.I. Torres Arza[139g], E. Torró Pastor[168], M. Toscani[31], C. Tosciri[40], M. Tost[11], D.R. Tovey[144], T. Trefzger[171], P.M. Tricarico[13], A. Tricoli[30], I.M. Trigger[161a], S. Trincaz-Duvoid[129], D.A. Trischuk[170], A. Tropina[39], D. Truncali[76a,76b], L. Truong[34c], M. Trzebinski[87], A. Trzupek[87], F. Tsai[150], M. Tsai[107], A. Tsiamis[157], P.V. Tsiareshka[39], S. Tsigaridas[161a], A. Tsirigotis[157,u], V. Tsiskaridze[154a], E.G. Tskhadadze[154a], Y. Tsujikawa[88], I.I. Tsukerman[38], V. Tsulaia[18a], S. Tsuno[83], K. Tsuri[120], D. Tsybychev[150], Y. Tu[64b], A. Tudorache[28b], V. Tudorache[28b], S.B. Tuncay[128], S. Turchikhin[57b,57a], I. Turk Cakir[3a], R. Turra[71a], T. Turtuvshin[39,ac], P.M. Tuts[42], S. Tzamarias[157,d], Y. Uematsu[83], F. Ukegawa[162], P.A. Ulloa Poblete[139c,139b], E.N. Umaka[30], G. Unal[37], A. Undrus[30], G. Unel[164], J. Urban[29b], P. Urrejola[139e], G. Usai[8], R. Ushioda[159], M. Usman[109], F. Ustuner[52], Z. Uysal[81], V. Vacek[134], B. Vachon[105], T. Vafeiadis[37], A. Vaitkus[97], C. Valderanis[110], E. Valdes Santurio[47a,47b], M. Valente[37], S. Valentinetti[24b,24a], A. Valero[168], E. Valiente Moreno[168], A. Vallier[90], J.A. Valls Ferrer[168], D.R. Van Arneman[116], A. Van Der Graaf[49], H.Z. Van Der Schyf[34j], P. Van Gemmeren[6], M. Van Rijnbach[37], S. Van Stroud[97], I. Van Vulpen[116], P. Vana[135], M. Vanadia[76a,76b], U.M. Vande Voorde[149], W. Vandelli[37], E.R. Vandewall[148], D. Vannicola[156], L. Vannoli[53], R. Vari[75a], M. Varma[177], E.W. Varnes[7], C. Varni[79], D. Varouchas[66], L. Varriale[168], K.E. Varvell[152], M.E. Vasile[28b], L. Vaslin[83], M.D. Vassilev[148], A. Vasyukov[39], L.M. Vaughan[123], R. Vavricka[135], T. Vazquez Schroeder[13], J. Veatch[32], V. Vecchio[102], M.J. Veen[104], I. Veliscek[30], I. Velkovska[94], L.M. Veloce[160], F. Veloso[132a,132c], A.G. Veltman[52], S. Veneziano[75a], A. Ventura[70a,70b], A. Verbytskyi[111],

M. Verducci[74a,74b], C. Vergis[95], M. Verissimo De Araujo[82b], W. Verkerke[116], J.C. Vermeulen[116], C. Vernieri[148], M. Vessella[164], M.C. Vetterli[147,ai], A. Vgenopoulos[101], N. Viaux Maira[139g,af], T. Vickey[144], O.E. Vickey Boeriu[144], G.H.A. Viehhauser[128], L. Vigani[63b], M. Vigl[111], M. Villa[24b,24a], M. Villaplana Perez[168], E.M. Villhauer[40], E. Vilucchi[53], M. Vincent[168], M.G. Vincter[35], A. Visibile[116], A. Visive[116], C. Vittori[37], I. Vivarelli[24b,24a], M.I. Vivas Albornoz[48], E. Voevodina[111], F. Vogel[110], J.C. Voigt[50], P. Vokac[134], Yu. Volkotrub[86b], L. Vomberg[25], E. Von Toerne[25], B. Vormwald[37], K. Vorobev[51], M. Vos[168], K. Voss[146], M. Vozak[37], L. Vozdecky[122], N. Vranjes[16], M. Vranjes Milosavljevic[16], M. Vreeswijk[116], N.K. Vu[143b,143a], R. Vuillermet[37], O. Vujinovic[101], I. Vukotic[40], I.K. Vyas[35], J.F. Wack[33], S. Wada[162], C. Wagner[148], J.M. Wagner[18a], W. Wagner[176], S. Wahdan[176], H. Wahlberg[91], C.H. Waits[122], J. Walder[136], R. Walker[110], K. Walkingshaw Pass[59], W. Walkowiak[146], A. Wall[130], E.J. Wallin[99], T. Wamorkar[18a], K. Wandall-Christensen[168], A. Wang[62], A.Z. Wang[138], C. Wang[48], C. Wang[11], H. Wang[18a], J. Wang[64c], P. Wang[102], P. Wang[97], R. Wang[61], R. Wang[6], S.M. Wang[153], S. Wang[14], T. Wang[115], T. Wang[62], W.T. Wang[128], W. Wang[14], X. Wang[167], X. Wang[143a], X. Wang[48], Y. Wang[150], Y. Wang[62], Z. Wang[107], Z. Wang[143b], Z. Wang[107], C. Wanotayaroj[83], A. Warburton[105], A.L. Warnerbring[146], S. Waterhouse[96], A.T. Watson[21], H. Watson[52], M.F. Watson[21], E. Watton[37], G. Watts[141], B.M. Waugh[97], J.M. Webb[54], C. Weber[30], M.S. Weber[20], S.M. Weber[63a], C. Wei[62], Y. Wei[54], A.R. Weidberg[128], E.J. Weik[119], J. Weingarten[49], C. Weiser[54], C.J. Wells[48], T. Wenaus[30], T. Wengler[37], N.S. Wenke[111], N. Wermes[25], M. Wessels[63a], A.M. Wharton[92], A.S. White[61], A. White[8], M.J. White[1], D. Whiteson[164], L. Wickremasinghe[126], W. Wiedenmann[175], M. Wielers[136], R. Wierda[149], C. Wiglesworth[43], H.G. Wilkens[37], J.J.H. Wilkinson[33], D.M. Williams[42], H.H. Williams[130], S. Williams[33], S. Willocq[104], B.J. Wilson[102], D.J. Wilson[102], P.J. Windischhofer[40], F.I. Winkel[31], F. Winklmeier[125], B.T. Winter[54], M. Wittgen[148], M. Wobisch[98], T. Wojtkowski[60], Z. Wolffs[116], J. Wollrath[37], M.W. Wolter[87], H. Wolters[132a,132c], M.C. Wong[138], E.L. Woodward[42], S.D. Worm[48], B.K. Wosiek[87], K.W. Woźniak[87], S. Wozniewski[55], K. Wraight[59], C. Wu[160], C. Wu[21], J. Wu[158], M. Wu[113b], M. Wu[115], S.L. Wu[175], S. Wu[14,ak], X. Wu[62], Y.Q. Wu[160], Y. Wu[62], Z. Wu[4], Z. Wu[113a], J. Wuerzinger[111], T.R. Wyatt[102], B.M. Wynne[52], S. Xella[43], L. Xia[113a], M. Xie[62], A. Xiong[125], D. Xu[14], H. Xu[62], L. Xu[62], R. Xu[130], T. Xu[107], W. Xu[113a], Y. Xu[141], Z. Xu[52], R. Xue[131], B. Yabsley[152], S. Yacoob[34a], Y. Yamaguchi[83], E. Yamashita[158], H. Yamauchi[162], T. Yamazaki[18a], Y. Yamazaki[85], S. Yan[59], Z. Yan[104], H.J. Yang[143a,143b], H.T. Yang[62], S. Yang[62], T. Yang[64c], X. Yang[37], X. Yang[14], Y. Yang[158], Y. Yang[62], W-M. Yao[18a], C.L. Yardley[151], J. Ye[14], S. Ye[30], X. Ye[62], Y. Yeh[97], I. Yeletskikh[39], B. Yeo[18b], M.R. Yexley[97], T.P. Yildirim[128], K. Yorita[173], C.J.S. Young[37], C. Young[148], I.N.L. Young[59], N.D. Young[125], Y. Yu[62], J. Yuan[14,113c], M. Yuan[107], R. Yuan[143b], L. Yue[97], M. Zaazoua[62], B. Zabinski[87], I. Zahir[36a], A. Zaio[57b,57a], Z.K. Zak[87], T. Zakareishvili[168], S. Zambito[56], J.A. Zamora Saa[139d], J. Zang[158], R. Zanzottera[71a,71b], O. Zaplatilek[134], C. Zeitnitz[176], H. Zeng[14], D.T. Zenger Jr[27], O. Zenin[38], T. Ženiš[29a], S. Zenz[95], D. Zerwas[66], D.F. Zhang[144], G. Zhang[14,ak], J. Zhang[142a], J. Zhang[6], L. Zhang[62], L. Zhang[113a], P. Zhang[14,113c],

R. Zhang[113a], S. Zhang[90], T. Zhang[158], Y. Zhang[141], Y. Zhang[97], Y. Zhang[62], Y. Zhang[113a], Z. Zhang[18a], Z. Zhang[142a], Z. Zhang[66], H. Zhao[141], T. Zhao[142a], Y. Zhao[35], Z. Zhao[62], Z. Zhao[62], A. Zhemchugov[39], J. Zheng[113a], K. Zheng[167], X. Zheng[62], Z. Zheng[148], D. Zhong[167], B. Zhou[107], B. Zhou[143b], H. Zhou[7], N. Zhou[143a], Y. Zhou[15], Y. Zhou[113a], Y. Zhou[7], J. Zhu[107], X. Zhu[143b], Y. Zhu[143a], Y. Zhu[62], X. Zhuang[14], K. Zhukov[68], N.I. Zimine[39], J. Zinsser[63b], M. Ziolkowski[146], L. Živković[16], A. Zoccoli[24b,24a], K. Zoch[61], A. Zografos[37], T.G. Zorbas[144], O. Zormpa[46], L. Zwalinski[37]

[1] *Department of Physics, University of Adelaide, Adelaide, Australia*
[2] *Department of Physics, University of Alberta, Edmonton AB, Canada*
[3a] *Department of Physics, Ankara University, Ankara, Türkiye*
[3b] *Division of Physics, TOBB University of Economics and Technology, Ankara, Türkiye*
[4] *LAPP, Université Savoie Mont Blanc, CNRS/IN2P3, Annecy, France*
[5] *APC, Université Paris Cité, CNRS/IN2P3, Paris, France*
[6] *High Energy Physics Division, Argonne National Laboratory, Argonne IL, U.S.A.*
[7] *Department of Physics, University of Arizona, Tucson AZ, U.S.A.*
[8] *Department of Physics, University of Texas at Arlington, Arlington TX, U.S.A.*
[9] *Physics Department, National and Kapodistrian University of Athens, Athens, Greece*
[10] *Physics Department, National Technical University of Athens, Zografou, Greece*
[11] *Department of Physics, University of Texas at Austin, Austin TX, U.S.A.*
[12] *Institute of Physics, Azerbaijan Academy of Sciences, Baku, Azerbaijan*
[13] *Institut de Física d'Altes Energies (IFAE), Barcelona Institute of Science and Technology, Barcelona, Spain*
[14] *Institute of High Energy Physics, Chinese Academy of Sciences, Beijing, China*
[15] *Physics Department, Tsinghua University, Beijing, China*
[16] *Institute of Physics, University of Belgrade, Belgrade, Serbia*
[17] *Department for Physics and Technology, University of Bergen, Bergen, Norway*
[18a] *Physics Division, Lawrence Berkeley National Laboratory, Berkeley CA, U.S.A.*
[18b] *University of California, Berkeley CA, U.S.A.*
[19] *Institut für Physik, Humboldt Universität zu Berlin, Berlin, Germany*
[20] *Albert Einstein Center for Fundamental Physics and Laboratory for High Energy Physics, University of Bern, Bern, Switzerland*
[21] *School of Physics and Astronomy, University of Birmingham, Birmingham, U.K.*
[22a] *Department of Physics, Bogazici University, Istanbul, Türkiye*
[22b] *Department of Physics Engineering, Gaziantep University, Gaziantep, Türkiye*
[22c] *Department of Physics, Istanbul University, Istanbul, Türkiye*
[23a] *Facultad de Ciencias y Centro de Investigaciónes, Universidad Antonio Nariño, Bogotá, Colombia*
[23b] *Departamento de Física, Universidad Nacional de Colombia, Bogotá, Colombia*
[24a] *Dipartimento di Fisica e Astronomia A. Righi, Università di Bologna, Bologna, Italy*
[24b] *INFN Sezione di Bologna, Italy*
[25] *Physikalisches Institut, Universität Bonn, Bonn, Germany*
[26] *Department of Physics, Boston University, Boston MA, U.S.A.*
[27] *Department of Physics, Brandeis University, Waltham MA, U.S.A.*
[28a] *Transilvania University of Brasov, Brasov, Romania*
[28b] *Horia Hulubei National Institute of Physics and Nuclear Engineering, Bucharest, Romania*
[28c] *Department of Physics, Alexandru Ioan Cuza University of Iasi, Iasi, Romania*
[28d] *National Institute for Research and Development of Isotopic and Molecular Technologies, Physics Department, Cluj-Napoca, Romania*
[28e] *National University of Science and Technology Politechnica, Bucharest, Romania*
[28f] *West University in Timisoara, Timisoara, Romania*
[28g] *Faculty of Physics, University of Bucharest, Bucharest, Romania*

JHEP01(2026)117

[29a] Faculty of Mathematics, Physics and Informatics, Comenius University, Bratislava, Slovak Republic
[29b] Department of Subnuclear Physics, Institute of Experimental Physics of the Slovak Academy of Sciences, Kosice, Slovak Republic
[30] Physics Department, Brookhaven National Laboratory, Upton NY, U.S.A.
[31] Universidad de Buenos Aires, Facultad de Ciencias Exactas y Naturales, Departamento de Física, y CONICET, Instituto de Física de Buenos Aires (IFIBA), Buenos Aires, Argentina
[32] California State University, CA, U.S.A.
[33] Cavendish Laboratory, University of Cambridge, Cambridge, U.K.
[34a] Department of Physics, University of Cape Town, Cape Town, South Africa
[34b] iThemba Labs, Western Cape, South Africa
[34c] Department of Mechanical Engineering Science, University of Johannesburg, Johannesburg, South Africa
[34d] National Institute of Physics, University of the Philippines Diliman, Philippines
[34j] School of Physics, University of the Witwatersrand, Johannesburg, South Africa
[35] Department of Physics, Carleton University, Ottawa ON, Canada
[36a] Faculté des Sciences Ain Chock, Université Hassan II de Casablanca, Morocco
[36b] Faculté des Sciences, Université Ibn-Tofail, Kénitra, Morocco
[36d] LPMR, Faculté des Sciences, Université Mohamed Premier, Oujda, Morocco
[36e] Faculté des sciences, Université Mohammed V, Rabat, Morocco
[36f] Institute of Applied Physics, Mohammed VI Polytechnic University, Ben Guerir, Morocco
[37] CERN, Geneva, Switzerland
[38] Affiliated with an institute formerly covered by a cooperation agreement with CERN
[39] Affiliated with an international laboratory covered by a cooperation agreement with CERN
[40] Enrico Fermi Institute, University of Chicago, Chicago IL, U.S.A.
[41] LPC, Université Clermont Auvergne, CNRS/IN2P3, Clermont-Ferrand, France
[42] Nevis Laboratory, Columbia University, Irvington NY, U.S.A.
[43] Niels Bohr Institute, University of Copenhagen, Copenhagen, Denmark
[44a] Dipartimento di Fisica, Università della Calabria, Rende, Italy
[44b] INFN Gruppo Collegato di Cosenza, Laboratori Nazionali di Frascati, Italy
[45] Physics Department, Southern Methodist University, Dallas TX, U.S.A.
[46] National Centre for Scientific Research "Demokritos", Agia Paraskevi, Greece
[47a] Department of Physics, Stockholm University, Sweden
[47b] Oskar Klein Centre, Stockholm, Sweden
[48] Deutsches Elektronen-Synchrotron DESY, Hamburg and Zeuthen, Germany
[49] Fakultät Physik, Technische Universität Dortmund, Dortmund, Germany
[50] Institut für Kern- und Teilchenphysik, Technische Universität Dresden, Dresden, Germany
[51] Department of Physics, Duke University, Durham NC, U.S.A.
[52] SUPA — School of Physics and Astronomy, University of Edinburgh, Edinburgh, U.K.
[53] INFN e Laboratori Nazionali di Frascati, Frascati, Italy
[54] Physikalisches Institut, Albert-Ludwigs-Universität Freiburg, Freiburg, Germany
[55] II. Physikalisches Institut, Georg-August-Universität Göttingen, Göttingen, Germany
[56] Département de Physique Nucléaire et Corpusculaire, Université de Genève, Genève, Switzerland
[57a] Dipartimento di Fisica, Università di Genova, Genova, Italy
[57b] INFN Sezione di Genova, Italy
[58] II. Physikalisches Institut, Justus-Liebig-Universität Giessen, Giessen, Germany
[59] SUPA — School of Physics and Astronomy, University of Glasgow, Glasgow, U.K.
[60] LPSC, Université Grenoble Alpes, CNRS/IN2P3, Grenoble INP, Grenoble, France
[61] Laboratory for Particle Physics and Cosmology, Harvard University, Cambridge MA, U.S.A.
[62] Department of Modern Physics and State Key Laboratory of Particle Detection and Electronics, University of Science and Technology of China, Hefei, China
[63a] Kirchhoff-Institut für Physik, Ruprecht-Karls-Universität Heidelberg, Heidelberg, Germany
[63b] Physikalisches Institut, Ruprecht-Karls-Universität Heidelberg, Heidelberg, Germany
[64a] Department of Physics, Chinese University of Hong Kong, Shatin, N.T., Hong Kong, China

[64b] *Department of Physics, University of Hong Kong, Hong Kong, China*
[64c] *Department of Physics and Institute for Advanced Study, Hong Kong University of Science and Technology, Clear Water Bay, Kowloon, Hong Kong, China*
[65] *Department of Physics, National Tsing Hua University, Hsinchu, Taiwan*
[66] *IJCLab, Université Paris-Saclay, CNRS/IN2P3, 91405, Orsay, France*
[67] *Centro Nacional de Microelectrónica (IMB-CNM-CSIC), Barcelona, Spain*
[68] *Department of Physics, Indiana University, Bloomington IN, U.S.A.*
[69a] *INFN Gruppo Collegato di Udine, Sezione di Trieste, Udine, Italy*
[69b] *ICTP, Trieste, Italy*
[69c] *Dipartimento Politecnico di Ingegneria e Architettura, Università di Udine, Udine, Italy*
[70a] *INFN Sezione di Lecce, Italy*
[70b] *Dipartimento di Matematica e Fisica, Università del Salento, Lecce, Italy*
[71a] *INFN Sezione di Milano, Italy*
[71b] *Dipartimento di Fisica, Università di Milano, Milano, Italy*
[72a] *INFN Sezione di Napoli, Italy*
[72b] *Dipartimento di Fisica, Università di Napoli, Napoli, Italy*
[73a] *INFN Sezione di Pavia, Italy*
[73b] *Dipartimento di Fisica, Università di Pavia, Pavia, Italy*
[74a] *INFN Sezione di Pisa, Italy*
[74b] *Dipartimento di Fisica E. Fermi, Università di Pisa, Pisa, Italy*
[75a] *INFN Sezione di Roma, Italy*
[75b] *Dipartimento di Fisica, Sapienza Università di Roma, Roma, Italy*
[76a] *INFN Sezione di Roma Tor Vergata, Italy*
[76b] *Dipartimento di Fisica, Università di Roma Tor Vergata, Roma, Italy*
[77a] *INFN Sezione di Roma Tre, Italy*
[77b] *Dipartimento di Matematica e Fisica, Università Roma Tre, Roma, Italy*
[78a] *INFN-TIFPA, Italy*
[78b] *Università degli Studi di Trento, Trento, Italy*
[79] *Universität Innsbruck, Department of Astro and Particle Physics, Innsbruck, Austria*
[80] *Department of Physics and Astronomy, Iowa State University, Ames IA, U.S.A.*
[81] *Istinye University, Sariyer, Istanbul, Türkiye*
[82a] *Departamento de Engenharia Elétrica, Universidade Federal de Juiz de Fora (UFJF), Juiz de Fora, Brazil*
[82b] *Universidade Federal do Rio De Janeiro COPPE/EE/IF, Rio de Janeiro, Brazil*
[82c] *Instituto de Física, Universidade de São Paulo, São Paulo, Brazil*
[82d] *Rio de Janeiro State University, Rio de Janeiro, Brazil*
[82e] *Federal University of Bahia, Bahia, Brazil*
[83] *KEK, High Energy Accelerator Research Organization, Tsukuba, Japan*
[84a] *Khalifa University of Science and Technology, Abu Dhabi, United Arab Emirates*
[84b] *University of Sharjah, Sharjah, United Arab Emirates*
[85] *Graduate School of Science, Kobe University, Kobe, Japan*
[86a] *AGH University of Krakow, Faculty of Physics and Applied Computer Science, Krakow, Poland*
[86b] *Marian Smoluchowski Institute of Physics, Jagiellonian University, Krakow, Poland*
[87] *Institute of Nuclear Physics Polish Academy of Sciences, Krakow, Poland*
[88] *Faculty of Science, Kyoto University, Kyoto, Japan*
[89] *Research Center for Advanced Particle Physics and Department of Physics, Kyushu University, Fukuoka, Japan*
[90] *L2IT, Université de Toulouse, CNRS/IN2P3, UPS, Toulouse, France*
[91] *Instituto de Física La Plata, Universidad Nacional de La Plata and CONICET, La Plata, Argentina*
[92] *Physics Department, Lancaster University, Lancaster, U.K.*
[93] *Oliver Lodge Laboratory, University of Liverpool, Liverpool, U.K.*
[94] *Department of Experimental Particle Physics, Jožef Stefan Institute and Department of Physics, University of Ljubljana, Ljubljana, Slovenia*

JHEP01(2026)117

[95] *Department of Physics and Astronomy, Queen Mary University of London, London, U.K.*
[96] *Department of Physics, Royal Holloway University of London, Egham, U.K.*
[97] *Department of Physics and Astronomy, University College London, London, U.K.*
[98] *Louisiana Tech University, Ruston LA, U.S.A.*
[99] *Fysiska institutionen, Lunds universitet, Lund, Sweden*
[100] *Departamento de Física Teorica C-15 and CIAFF, Universidad Autónoma de Madrid, Madrid, Spain*
[101] *Institut für Physik, Universität Mainz, Mainz, Germany*
[102] *School of Physics and Astronomy, University of Manchester, Manchester, U.K.*
[103] *CPPM, Aix-Marseille Université, CNRS/IN2P3, Marseille, France*
[104] *Department of Physics, University of Massachusetts, Amherst MA, U.S.A.*
[105] *Department of Physics, McGill University, Montreal QC, Canada*
[106] *School of Physics, University of Melbourne, Victoria, Australia*
[107] *Department of Physics, University of Michigan, Ann Arbor MI, U.S.A.*
[108] *Department of Physics and Astronomy, Michigan State University, East Lansing MI, U.S.A.*
[109] *Group of Particle Physics, University of Montreal, Montreal QC, Canada*
[110] *Fakultät für Physik, Ludwig-Maximilians-Universität München, München, Germany*
[111] *Max-Planck-Institut für Physik (Werner-Heisenberg-Institut), München, Germany*
[112] *Graduate School of Science and Kobayashi-Maskawa Institute, Nagoya University, Nagoya, Japan*
[113a] *Department of Physics, Nanjing University, Nanjing, China*
[113b] *School of Science, Shenzhen Campus of Sun Yat-sen University, China*
[113c] *University of Chinese Academy of Science (UCAS), Beijing, China*
[114] *Department of Physics and Astronomy, University of New Mexico, Albuquerque NM, U.S.A.*
[115] *Institute for Mathematics, Astrophysics and Particle Physics, Radboud University/Nikhef, Nijmegen, Netherlands*
[116] *Nikhef National Institute for Subatomic Physics and University of Amsterdam, Amsterdam, Netherlands*
[117] *Department of Physics, Northern Illinois University, DeKalb IL, U.S.A.*
[118a] *New York University Abu Dhabi, Abu Dhabi, United Arab Emirates*
[118b] *United Arab Emirates University, Al Ain, United Arab Emirates*
[119] *Department of Physics, New York University, New York NY, U.S.A.*
[120] *Ochanomizu University, Otsuka, Bunkyo-ku, Tokyo, Japan*
[121] *Ohio State University, Columbus OH, U.S.A.*
[122] *Homer L. Dodge Department of Physics and Astronomy, University of Oklahoma, Norman OK, U.S.A.*
[123] *Department of Physics, Oklahoma State University, Stillwater OK, U.S.A.*
[124] *Palacký University, Joint Laboratory of Optics, Olomouc, Czech Republic*
[125] *Institute for Fundamental Science, University of Oregon, Eugene, OR, U.S.A.*
[126] *Graduate School of Science, University of Osaka, Osaka, Japan*
[127] *Department of Physics, University of Oslo, Oslo, Norway*
[128] *Department of Physics, Oxford University, Oxford, U.K.*
[129] *LPNHE, Sorbonne Université, Université Paris Cité, CNRS/IN2P3, Paris, France*
[130] *Department of Physics, University of Pennsylvania, Philadelphia PA, U.S.A.*
[131] *Department of Physics and Astronomy, University of Pittsburgh, Pittsburgh PA, U.S.A.*
[132a] *Laboratório de Instrumentação e Física Experimental de Partículas — LIP, Lisboa, Portugal*
[132b] *Departamento de Física, Faculdade de Ciências, Universidade de Lisboa, Lisboa, Portugal*
[132c] *Departamento de Física, Universidade de Coimbra, Coimbra, Portugal*
[132d] *Centro de Física Nuclear da Universidade de Lisboa, Lisboa, Portugal*
[132e] *Departamento de Física, Escola de Ciências, Universidade do Minho, Braga, Portugal*
[132g] *Departamento de Física, Instituto Superior Técnico, Universidade de Lisboa, Lisboa, Portugal*
[133] *Institute of Physics of the Czech Academy of Sciences, Prague, Czech Republic*
[134] *Czech Technical University in Prague, Prague, Czech Republic*
[135] *Charles University, Faculty of Mathematics and Physics, Prague, Czech Republic*
[136] *Particle Physics Department, Rutherford Appleton Laboratory, Didcot, U.K.*
[137] *IRFU, CEA, Université Paris-Saclay, Gif-sur-Yvette, France*
[138] *Santa Cruz Institute for Particle Physics, University of California Santa Cruz, Santa Cruz CA, U.S.A.*

JHEP01(2026)117

[139a] *Departamento de Física, Pontificia Universidad Católica de Chile, Santiago, Chile*
[139b] *Millennium Institute for Subatomic physics at high energy frontier (SAPHIR), Santiago, Chile*
[139c] *Instituto de Investigación Multidisciplinario en Ciencia y Tecnología, y Departamento de Física, Universidad de La Serena, Chile*
[139d] *Universidad Andres Bello, Department of Physics, Santiago, Chile*
[139e] *Universidad San Sebastian, Recoleta, Chile*
[139f] *Instituto de Alta Investigación, Universidad de Tarapacá, Arica, Chile*
[139g] *Departamento de Física, Universidad Técnica Federico Santa María, Valparaíso, Chile*
[140] *Department of Physics, Institute of Science, Tokyo, Japan*
[141] *Department of Physics, University of Washington, Seattle WA, U.S.A.*
[142a] *Institute of Frontier and Interdisciplinary Science and Key Laboratory of Particle Physics and Particle Irradiation (MOE), Shandong University, Qingdao, China*
[142b] *School of Physics, Zhengzhou University, China*
[143a] *State Key Laboratory of Dark Matter Physics, School of Physics and Astronomy, Shanghai Jiao Tong University, Key Laboratory for Particle Astrophysics and Cosmology (MOE), SKLPPC, Shanghai, China*
[143b] *State Key Laboratory of Dark Matter Physics, Tsung-Dao Lee Institute, Shanghai Jiao Tong University, Shanghai, China*
[144] *Department of Physics and Astronomy, University of Sheffield, Sheffield, U.K.*
[145] *Department of Physics, Shinshu University, Nagano, Japan*
[146] *Department Physik, Universität Siegen, Siegen, Germany*
[147] *Department of Physics, Simon Fraser University, Burnaby BC, Canada*
[148] *SLAC National Accelerator Laboratory, Stanford CA, U.S.A.*
[149] *Department of Physics, Royal Institute of Technology, Stockholm, Sweden*
[150] *Departments of Physics and Astronomy, Stony Brook University, Stony Brook NY, U.S.A.*
[151] *Department of Physics and Astronomy, University of Sussex, Brighton, U.K.*
[152] *School of Physics, University of Sydney, Sydney, Australia*
[153] *Institute of Physics, Academia Sinica, Taipei, Taiwan*
[154a] *E. Andronikashvili Institute of Physics, Iv. Javakhishvili Tbilisi State University, Tbilisi, Georgia*
[154b] *High Energy Physics Institute, Tbilisi State University, Tbilisi, Georgia*
[154c] *University of Georgia, Tbilisi, Georgia*
[155] *Department of Physics, Technion, Israel Institute of Technology, Haifa, Israel*
[156] *Raymond and Beverly Sackler School of Physics and Astronomy, Tel Aviv University, Tel Aviv, Israel*
[157] *Department of Physics, Aristotle University of Thessaloniki, Thessaloniki, Greece*
[158] *International Center for Elementary Particle Physics and Department of Physics, University of Tokyo, Tokyo, Japan*
[159] *Graduate School of Science and Technology, Tokyo Metropolitan University, Tokyo, Japan*
[160] *Department of Physics, University of Toronto, Toronto ON, Canada*
[161a] *TRIUMF, Vancouver BC, Canada*
[161b] *Department of Physics and Astronomy, York University, Toronto ON, Canada*
[162] *Division of Physics and Tomonaga Center for the History of the Universe, Faculty of Pure and Applied Sciences, University of Tsukuba, Tsukuba, Japan*
[163] *Department of Physics and Astronomy, Tufts University, Medford MA, U.S.A.*
[164] *Department of Physics and Astronomy, University of California Irvine, Irvine CA, U.S.A.*
[165] *University of West Attica, Athens, Greece*
[166] *Department of Physics and Astronomy, University of Uppsala, Uppsala, Sweden*
[167] *Department of Physics, University of Illinois, Urbana IL, U.S.A.*
[168] *Instituto de Física Corpuscular (IFIC), Centro Mixto Universidad de Valencia — CSIC, Valencia, Spain*
[169] *Department of Physics, University of British Columbia, Vancouver BC, Canada*
[170] *Department of Physics and Astronomy, University of Victoria, Victoria BC, Canada*
[171] *Fakultät für Physik und Astronomie, Julius-Maximilians-Universität Würzburg, Würzburg, Germany*
[172] *Department of Physics, University of Warwick, Coventry, U.K.*
[173] *Waseda University, Tokyo, Japan*
[174] *Department of Particle Physics and Astrophysics, Weizmann Institute of Science, Rehovot, Israel*

JHEP01(2026)117

[175] Department of Physics, University of Wisconsin, Madison WI, U.S.A.
[176] Fakultät für Mathematik und Naturwissenschaften, Fachgruppe Physik, Bergische Universität Wuppertal, Wuppertal, Germany
[177] Department of Physics, Yale University, New Haven CT, U.S.A.
[178] Yerevan Physics Institute, Yerevan, Armenia

[a] Also at Affiliated with an institute formerly covered by a cooperation agreement with CERN
[b] Also at An-Najah National University, Nablus, Palestine
[c] Also at Borough of Manhattan Community College, City University of New York, New York NY, U.S.A.
[d] Also at Center for Interdisciplinary Research and Innovation (CIRI-AUTH), Thessaloniki, Greece
[e] Also at Centre of Physics of the Universities of Minho and Porto (CF-UM-UP), Portugal
[f] Also at CERN, Geneva, Switzerland
[g] Also at Département de Physique Nucléaire et Corpusculaire, Université de Genève, Genève, Switzerland
[h] Also at Departament de Fisica de la Universitat Autonoma de Barcelona, Barcelona, Spain
[i] Also at Department of Financial and Management Engineering, University of the Aegean, Chios, Greece
[j] Also at Department of Mathematical Sciences, University of South Africa, Johannesburg, South Africa
[k] Also at Department of Modern Physics and State Key Laboratory of Particle Detection and Electronics, University of Science and Technology of China, Hefei, China
[l] Also at Department of Physics, Bolu Abant Izzet Baysal University, Bolu, Türkiye
[m] Also at Department of Physics, King's College London, London, U.K.
[n] Also at Department of Physics, Stanford University, Stanford CA, U.S.A.
[o] Also at Department of Physics, Stellenbosch University, South Africa
[p] Also at Department of Physics, University of Fribourg, Fribourg, Switzerland
[q] Also at Department of Physics, University of Thessaly, Greece
[r] Also at Department of Physics, Westmont College, Santa Barbara, U.S.A.
[s] Also at Faculty of Physics, Sofia University, 'St. Kliment Ohridski', Sofia, Bulgaria
[t] Also at Faculty of Physics, University of Bucharest, Romania
[u] Also at Hellenic Open University, Patras, Greece
[v] Also at Henan University, China
[w] Also at Imam Mohammad Ibn Saud Islamic University, Saudi Arabia
[x] Also at Institucio Catalana de Recerca i Estudis Avancats, ICREA, Barcelona, Spain
[y] Also at Institut für Experimentalphysik, Universität Hamburg, Hamburg, Germany
[z] Also at Institute for Nuclear Research and Nuclear Energy (INRNE) of the Bulgarian Academy of Sciences, Sofia, Bulgaria
[aa] Also at Institute of Applied Physics, Mohammed VI Polytechnic University, Ben Guerir, Morocco
[ab] Also at Institute of Particle Physics (IPP), Canada
[ac] Also at Institute of Physics and Technology, Mongolian Academy of Sciences, Ulaanbaatar, Mongolia
[ad] Also at Institute of Physics, Azerbaijan Academy of Sciences, Baku, Azerbaijan
[ae] Also at Institute of Theoretical Physics, Ilia State University, Tbilisi, Georgia
[af] Also at Millennium Institute for Subatomic physics at high energy frontier (SAPHIR), Santiago, Chile
[ag] Also at National Institute of Physics, University of the Philippines Diliman (Philippines), Philippines
[ah] Also at The Collaborative Innovation Center of Quantum Matter (CICQM), Beijing, China
[ai] Also at TRIUMF, Vancouver BC, Canada
[aj] Also at Università di Napoli Parthenope, Napoli, Italy
[ak] Also at University of Chinese Academy of Sciences (UCAS), Beijing, China
[al] Also at University of Colorado Boulder, Department of Physics, Colorado, U.S.A.
[am] Also at University of Sienna, Italy
[an] Also at Washington College, Chestertown, MD, U.S.A.
[ao] Also at Yeditepe University, Physics Department, Istanbul, Türkiye
[†] Deceased

JHEP01(2026)117